Heritage Science

RESEARCH

Open Access

Influences of bulk structure of Calcarenitic rocks on water storage and transfer in order to assess durability and climate change impact.

UNESCO world heritage sites in Alexandria, Egypt

Sayed Hemeda[1*]

Abstract

The main purpose of this study is to understand influences of bulk structure of geomaterials on water storage and transfer, in order to assess durability and climate change impact on the UNESCO world heritage sites in Alexandria, Egypt. This study deals with the responses of water towards the physiochemical and physicomechanical behaviours of Calcarenitic rocks, that are utilized in Greek and Roman monuments at Alexandria. Many vulnerable archaeological sites [2.3–2.5 m above mean sea level (M.S.L)] are identified at Alexandria, specifically at the Eastern Harbor, El-Shatby the Greek necropolis and Moustafa Kamil Roman tombs and addition to the Roman Catacombs of Kom El-Shoqafa which excavated with deepth – 18 m from the land surface. These UNESCO heritage sites suffer climate change impact (heavy rains and sea water rising) as well as multiple geoenvironmental and geophysical hazards. In this study a general outline of the various tests, surveys and analyses is presented, highlighting the most important issues related to the durability and climate change impact. This paper represents the comprehensive in-situ, field and laboratory surveys and tests undertaken in these outstanding world heritage sites. The field testing program comprises various geotechnical and geophysical field and laboratory tests aiming to define the physical, mechanical and dynamic properties of the hard soils/soft rock materials of the archaeological sites where these outstanding monuments are excavated and constracted. By analysis of linear correlations, some essential mechanisms should be underlined, which may connect the macrostructure to the microstructure of the geomaterial. A systematic method of analysis clearly appeared and emphasized the role of the bulk structure (i.e. grain size, grain contact, specific area, pore shape and microporosity) on petrophysical and petromechanical behavior of rock materials. The study revealed that the petrophysical and geomechanical properties of Calcarenitic rocks are influenced by size, shape, packing of grains, porosity, cement and matrix content, all controlled strongly by depositional fabric and postdepositional processes. The accurate analysis of the physiochemical and physicomechanical behaviours of Calcarenitic rocks that are utilized in Greek and Roman monuments at Alexandria allowed us to define the pathology of these monuments and to estimate the durability, climate change impact and ultimate geostatic loads that they can survive under their present geoenvironmental conditions.

Keywords Climate change impact, Petrophysical properties, Petro-mechanical properties, Textural parameters, Geotechnical, Calcarenitic rocks, Cultural heritage, Archaeological sites, Greek and Roman monuments, Archaeological sites in Alexandria, Egypt

*Correspondence:
Sayed Hemeda
Sayed.hemeda@cu.edu.eg
Full list of author information is available at the end of the article

Introduction

The City of Alexandria is one of the most important UNESCO World heritage sites, which is inscribed on the UNESCO heritage preservation lists in the Mediterranean Sea. Alexandria city is at risk of coastal flooding and erosion due to sea level rise resulting from global warming. Alexandria, the bride of the Mediterranean, is listed among the 15 of the world's 20 coastal megacities that are at risk from S.L.R and coastal surges. Concerning the inundation scenario, the submergence would take place in the east and middle of Alexandria, but natural and artificial barriers would restrain the flooding to penetrate so far. While western Alexandria is relatively preserved by coastal sand dunes and ridges, and steep land slope.

Alexandria has experienced extreme events including storm surges and sea immersion. In the year 1303 AD, Alexandria was struck by a 9 m destructive tsunami wave after 40 min of strong seismic tremors. The disaster affected the area with a sudden rise in the sea-level [1]. Moreover, Alexandria City is unstable due to readjustment from substantial down warping of the thick superposed sequences of Nile Delta sediments, [2]. The observations of the sea-level in Alexandria show a relative sea-level rise of 2.9 mm/year to the mean sea-level. This value was extracted from tide gauge, archaeological data, and Radiocarbon core samples, [3, 4].

Alexandria is facing several hazardous environmental phenomena, particularly pluvial flash flooding, Sea level rise (S.L.R) and land subsidence. It has been considered to be one of the mediterranean cities most likely to be affected by sea level rise S.L.R because of the low elevation of the northern coastal zone. The high-elevated coastal ridges underlying Alexandria's seafront—maximum elevation of 12 m above M.S.L in addition to other protection elements are acting together as a natural quasi-barrier to mitigate sea flooding that may in turn affect the historical low-lying depressions located east and southeast of the city, where the archaeological sites under investigation are excavated and located.

Climate change leads to an increase in the number of natural disasters and their devastating impact on our natural and cultural heritage sites in Alexandria, Egypt.

The increase in the number of natural disasters related to climate change crises has exposed the Alexandrian cultural and natural heritage to a greater danger than ever before, which imposes new challenges on us to preserve the urban historic fabric and the built heritage in Egypt.

The United Nations (UN) Educational, Scientific and Cultural Organization UNESCO said in its new report that, the Mediterranean and nearby cities will be deeply affected by a tsunami that may arise. Saying that Marseille, Alexandria and Istanbul are in danger, the organization stated that the probability of a tsunami higher than one meter in the next 30 years is almost 100 percent, [5]. As shown in Fig. 1, Alexandria being hit by a tsunami in February 7, 2023 after a 7.8-magnitude earthquake struck Turkey and Syria, killing hundreds of people.

All subterranean monumental structures in Alexandria sufer from a common problem: water leakage. Over time, the infltration may lead to increased humidity to excessive levels within the void created by the structure.

This moisture and water seepage within the structure caused cracking and peeling of rock surface layers, the formation of salt blooms in addition to the sub-fuorescences that can be dangerous to wall paint layers. The interaction of moisture with carbon dioxide may further degrade, resulting in the potential leakage of unwanted gases or dangerous chemicals from the surrounding soil.

The underground Greek and Roman monuments at Alexandria are all excavated in the plioquaternary Calcarenitic rocks, that constitutes the basement of the whole region. A few kilometers to the north of the city, quarries still provide this ornamental rock widely used by stone craftsmen. It is characterized by variable and high porosity (18–47%) and thus an elevated permeability, and generally bad geotechnical quality. Its chemical composition

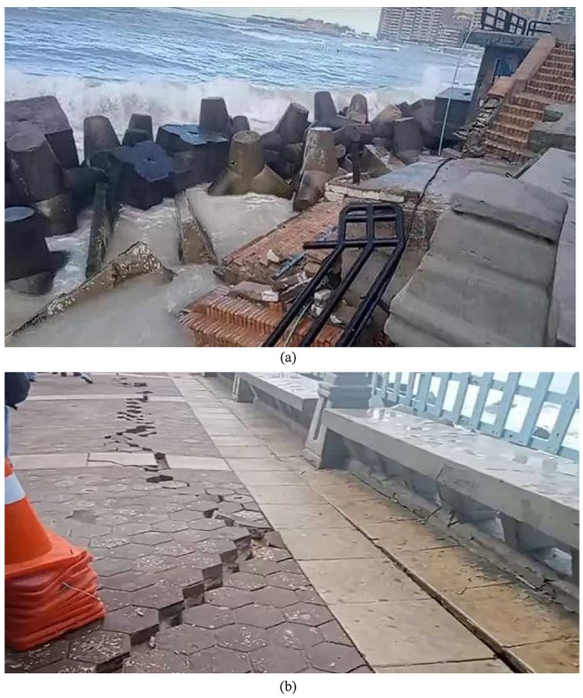

Fig. 1 Alexandria being hit by a tsunami in February 7, 2023 after a 7.8-magnitude earthquake struck Turkey and Syria, killing hundreds of people

is very rich in calcium carbonates and its rough surface allows a high receptivity to the atmospheric gaseous pollutants and to hydrous marine sprays and sea water charged with various salts.

The main purpose of this study is to understand influences of bulk structure of materials on water storage and transfer in order to assess durability and climate change impact. The study deals with the responses of water towards the physiochemical and physicomechanical behaviours of Calcarenitic rocks, that are utilized in Greek and Roman monuments at Alexandria.

The presence of water inside the porous matrix of rock materials plays a main role in determining their mechanical performance and stability. As well known, salt crystallization and transportation of unwanted substances through water penetration can lead to the formation of cracks and plane distortions, which strongly affecting the structural integrity of the construction itself. Stone durability is a term describing how well the material retains its original physical and mechanical properties. As a consequence, it concerns several aspects such as texture, structure, and mineralogical composition, as well as methods of quarrying and handling, applied loads, and environmental conditions to which the considered stone has been exposed. In particular, during the past few centuries, porous calcareous stones were extensively used as building material in several areas of Alexandria as apart of the mediterranean basin. In this coastal urban environments, after a protracted period of exposure to heavy rains, flash flooding and the atmospheric agents, these lithotypes are very often subjected to extensive crumbling due to soluble salt crystallization in pore spaces. Consequently, for this type of natural building material, the relationship among pore structure, water/moisture transport, and salt crystallization has been extensively investigated for understanding the mechanisms and kinetics of degradation processes, [6]. Calcarenite is used mainly for various purposes in the building industry, for the renovation of historical monuments, stonework, sculptures etc. Limestones are used as facing material and for the restoration of historical buildings.

Permeability and porosity have an impact on rock weathering, which affects the field of engineering utilization.

Porosity is one of the rock properties that are necessary for considering the solving of hydrological and hydrogeological problems by methods of numerical and physical modelling, [7].

By analysis of linear correlations, some essential mechanisms should be underlined, which may connect the macrostructure to the microstructure of the material. A systematic method of analysis should clearly appear and emphasize the role of the bulk structure (which includes the grain size, grain contact and pore shape) on petrophysical and petromechanical behavior of rock materials.

The main parameters leading to weathering should then be identified and models of correlations drawn. Correlations between the various physico-mechanical properties could ameliorate the possibilities to assess durability and weathering in the natural environment.

Study of these construction rock materials provides information about the origin, texture, distribution and composition which is used in the description of physiochemical and physio-mechanical properties, where the contolloing factors in the physiochemical and physiomechanical properties of the Calcarenitic rocks are primarly composition, environment of deposition, microstructure characters, and physical properties, [8].

The high-elevated coastal ridges underlying Alexandria's seafront with maximum elevation of 12 m above M.S.L, in addition to other protection elements are acting together as a natural quasi-barrier to mitigate sea flooding that may in turn affect the historical low-lying depressions located east and southeast of the city, [9].

Nowadays, it becomes a fact that the Earth suffered a global warming phenomenon, in the last couple of centuries, with serious environmental and economic hazards. One such crucial hazard is the accelerating Sea Level Rise (S.R.L) worldwide that causes sea flooding, particularly for low-elevation lands and coasts. According to the Intergovernmental Panel on Climate Change (IPCC), three chief remarks should be considered: (1) the global SRL has increased from 1.4 mm/year over the period 1901–1990 to 2.1 mm/year over 1970–2015 to 3.2 mm/year over 1993–2015 to 3.6 mm/year over 2006–2015, (2) under some specific scenarios, the global SRL could likely reach 0.84 m (0.61–1.10 m) by 2100 over the 1986–2005 level, and (3) if global warming is fast accelerating and the global air temperature is kept rising over the next three centuries, a global S.R.L could be over few meters by 2300. On another hand, it has been found that atmospheric pressure affects the sea level changes on a global basis over a long time. Moreover, warm air temperature could contribute significantly to the generation of severe sea level changes and storm surges in coastal regions [10].

In recent years, many researchers have focused on the relationship between textural parameters and petrophysical-mechanical properties of rocks and building materials, and several methods have been developed for a qualitative and quantitative evaluation of geometry and topology of pore network, pore size distribution, and grain size and shape. Physical properties include, above all, heat and fluid flows of engineering and geoscientific interest, indispensable to predicting the movement of hydrocarbons in a reservoir, the transport of

contaminants in an underground aquifer or weathering processes and stone decay in numerous architectural structures and historical monuments. Previous works on textural parameters that affect physical response have been presented by a few numbers of authors.

The rock materials used in this study are Calcarenite. The Calcarenite is a kind of sedimentary rock and widely used in many fields, such as civil construction, and renovation of historical monuments, stones and sculptures. This sedimentary rock in yellow ocher color is found mainly in the North coast of Egypt, and it was used for the construction and restoration of various historical monuments of Alexandria. It is characterized by high porosity (18–47%) and elevated permeability, [11]. Petrophysical and geomechanical properties of sedimentary rocks are influenced by size, shape, and packing of grains, porosity, cement and matrix content, all controlled strongly by depositional fabric and post depositional processes. Because of their geologic complexity, hydrocarbon reservoirs have become a widely discussed frontier in science and engineering, [12, 13]. Although permeability is a well-established property when considering relatively uniform porous media, its precise dependence on complex geometries and topologies such as those of carbonate rocks is still not well understood. Ref. [14] mentioned that pore-scale modeling, based on microCT images, allows direct identification and quantification of parameters related to pore structure and fluid properties for linking the fluid rock flow properties with geological information and establishing reliable rock classes.

Limestone members along the coastal ridge of Alexandria

Alexandria is built on a narrow coastal plain of Pleistocene carbonate sand ridges of 8–10 m elevation. These ridges extend westward parallel to the present coast.

The coastline in backed to the south by a series of different land use/ cover units:

Carbonate ridge, Maryut Lake, Inland depression, Drain, Desert, Urban, Industries, Agriculture and Architecture.

The exposed rocks in the northwest Mediterranean coastal zone are entirely of sedimentary origin ranging from early Miocene to Holocene with a maximum thickness of about 200 m. The surface deposits in Alexandria belong essentially to the Quaternary which are: 1- Holocene deposits, 2- Pleistocene deposits. The Tertiary deposits are represented as Pliocene and Miocene south of Alexandria [15–17].

The main geomorphologic units of Alexandria include major five units: 1- Coastal plain, which includes the Young, old and Piedmont plains, 2- Tableland 3- Aggredational depression, 4- Deltaic plain, and the 5- Brackish lagoons which includes the Maryut lake and Idku lake. The Young plain includes the degradation shore and aggradations shore. The Old plain includes the Inland ridges, depressions and underwater ridges.

For the Ridges; they run parallel to the coast in the backshore from Alexandria to Salum. The 1st coastal ridge is running from El Agami to El Salum, with width 400 m and height 20 m, which is oolitic sand. The 2nd is the El Max-Abu Qir ridge, which located south of first ridge with width 800 m and height 20–50 m, and consist mainly from chalky. The 3rd ridge is the Gebel Maryut ridge with 35–50 m height. The 4th ridge is the Khashm El Eish ridge. The 5th ridge is the oldest, Alam Shaltut-Alam El Afrag ridge. These ridges are missing/deformed at some localities due to local structures and erosion. Ridges represent ancient shoreline of Mediterranean during Pleistocene with elevation ranges from 10 to100 m.

For the Depressions; the 1st "coastal" depression is invaded by tidal sea water. The 2nd is "El Dekheila—Abu Sir" depression which is laying between 1 and 2. The 3rd is "Mallahet Maryut" depression. For the Stratigraphic units; the exposed rocks in the northwestern Mediterranean coastal zone are entirely sedimentary origin ranging from early Miocene to Holocene with maximum thickness of about 200 m. The surface deposits in Alexandria belong essentially to the Quaternary which are Holocene deposits and Pleistocene deposits. The Tertiary deposits are represented as Pliocene and Miocene south of Alexandria [17].

Alexandria province has shoreline, which extends for about 38 km between El-Agami headland to the west and Abu Qir headland to the east.

For the major historical and recent earthquakes in Alexandria, can be summarized as follow:

Alexandria city has experienced about (25) damaging earthquakes spanning the period 320 to 2000. (9) of (25) are located local offshore of Alexandria with average magnitudes (Ms = 6.7) & intensity IX MSK scale & time of shaking (2–3) sec. Other (14) were located mainly in the eastern Mediterranean region (i.e. Hellenic ARC), Ms (7.8) & intensity VI & time of shaking (3) sec. The most sever events include the 320 AD, 365 AD and 1303 AD earthquakes, where two of these destructive quakes destroyed 50,000 houses and killed 5000 people in Alexandria. Events, which are located as far as the red sea and gulf of Aqaba, are felt in Alexandria but without damage (ex.) 1969, 1995, Ms (6.9, 7.3 respectively), [18–22].

The exposed rock units belong to Alexandria formation are the Pleistocene and Younger quaternary. Litho logically it is composed of Oolitic detrital limestone building a number of elongated bar to the coast, laggonal marl and gypsum in depression and separating the Calcarenitic

bars. The carbonate granules are formed under water and transported in and by the retreat of sea and by section of wind. They represent fossil off—shore bars.

The stratigraphic sequence in Alexandria is difficult to be studied, where there is no rock exposure in Alexandria but great attention was given to different studies dealing with the geology, hydrology, geomorphology and economics of the northwestern coastal zone of Egypt.

Geological and hydro geological investigations on the Mediterranean coastal zone west of Alexandria include the work of [23–28] and others.

Vicente et al. [29] identified four ridges separated by three longitudinal valleys in between discussed the geology of the coastal zone, where El-Shatby Necropolis and the Necropolis of Mustafa Kamil are excavated. He ascribed a marine origin and Pliocene age to those ridges.

Shreadah et al. [30] and Doehne [31] noted that these ridges are made of fossiliferous oolitic limestone with foraminifera, pelecypods and gastropods. He also ascribed a marine origin to the ridges and considered them to represent bars cutting of lagoons.

Shaaban [8] noted that the Lake Mariut (LM) is an inland closed shallow lake (with a mean depth of 1 m) that lies south of Alexandria City. It is a depression that extends for about 20 km between 31°01′48″ and 31°10′30″N and 29°49′48″ and 29°57′00″E. Its bottom is below the sea level by value about 3.25 m and separated from the neighboring Mediterranean Sea by a ridge called Abuser. The lake (LM) is artificially subdivided into four principal basins by Desert Road and Umum Drain (UD; Omum, Umoum, El-Ommum). Maryut area is characterized by intensely white dunes formed by the piling up of a vast number of small rounded oolitic grains and unite to form masses of more compacted rocks. They ascribed a wind origin to these ridges, calling them wind-formed deposits.

Arnold and Zehnder [32] noted that many of these coast dunes near the west of the delta appear, in the main, to be composed of broken fragments of seashells, which on being heaped up and consolidated, produce the limestones employed as building material.

Zehnder [33] decided the no marine origin of these ridges.

Ashton [34] described the ridges as stretches of consolidated coastal bars separating ancient lagoon floors. He identified a sequence of ten ancient bars ranging in age from sililian to recent.

Basheer et al. [35], considered the ridges to represent old dunes, the material of which was derived from beach deposits.

El-Sayed et al. [36] described the most northern ridge as an "embryonic" friable dune, that represents the first stage in the evolution of these ridges. The third stage is a mature hardened ridge with a thick recrystallized top layer and a hard core. He attributed them to wind action.

Chalari et al. [37] studied the geology of the Pleistocene sediments of the Mediterranean coast west of Abu Qir town. They noted that they are present in the form of sand bars separated by seven lagoons are discerned. The bars are dated from pre-Roman to Sicilian according to their elevation and are considered as marine in origin.

El-Assal [38] studied the northern coast of the western desert of Egypt from Alexandria to El-Salum, and indicated that has been one of vigorous productivity of carbonate sedimentation during the quaternary and the quaternary carbonate dune, facies overlying Miocene facies, that are exposed on ground surface distant from the Mediterranean sea coast (i.e. to the south). The quaternary facies are four ridges, namely: ridge 1, 2, 3 and 4 arranged from the coast (the youngest) to inland (the oldest ridge) parallel to the present day sea coast with facies types as follow:

> Ridge 1: it is on the Mediterranean Sea coast, 5–10 m above sea level, Oolitic limestone, less cemented, isopachous cement indicate fresh water, phreatic zone. Most of Ooids are micritized, 1.4% quartz grain, porosity is high 25% to 40 percentages, Fe_2O_3 is 0.14%, CaO is 51.8%, and its facies are Oolitic bioclasts grainstone to packstone.
>
> Ridge 2: it is Oolitic bioclasts grainstone to packstone, it is moderately cemented by isopachous cement microspare or drusy sparite. It is 20–25 m height above sea level. The digenesis indicate fresh water meteoric environment, its SiO_2 is 1.3%, Fe_2O_3 is 0.16%, and CaO is 52.5%.
>
> Ridge 3: it is foraminiferal molluscal packstone; it is 35–44 m height above sea level. This bioclasts have thick micrite envelope and some skeletal parts are completely micritized forming peloids. It is a well-cemented rock, SiO_2 is 2.04%, Fe_2O_3 is 0.25%, and CaO is 51.5%.
>
> Ridge 4: it is algal bioclastic grainstone to packstone. Its SiO_2 is 4.04%, Fe_2O_3 is 0.39%, and CaO is 50.4%. It is 55–65 m above the sea level.

In this study, Table 1. Represents the Succession of beds in the coastal ridge of Alexandria.

The limestone of the four ridges differs chemically and physically from one ridge to the other. Rock of the coastal ridge has a limited thickness and weak lithification. They are used mainly for building purposes, specially the houses built on the coastal stretch. It is more convenient

for the owners to make use of the local material namely the limestones of the coastal ridge.

The succession of beds in the coastal ridge, in the studied stretch can be classified both according to surface outcrops, and subsurface sections from the excavated water wells into Pleistocene limestone and recent deposits. This classification includes only the limestones above water level. The investigated limestones can be differentiated into two members; The upper member with thickness 2 to 7.5 m is Oolitic intraclastic limestone. It is yellowish white upwards becoming brownish yellow downwards. It is fine to coarse grained with friable with spherical algal flora and pumice. The upper part of this member is fractured and rich in voids and cavities, especially the topmost two meters. At Abou youssef area, these voids and cavities are filled with ball like spherical shaped algal flora, representing reworked algal stems. In addition, pumice horizon is found at 5.7 m depth embedded in the limestone and occupying a thickness of about 10 cm. They are grey to yellowish grey in colour with different diameters ranging from 1 × 1 to 6 × 7 cm. The Basal member, the thickness is 4.5 m. It is skeletal sandy argilletic limestone. Brownish in color and friable [39].

Materials and methodology

Materials Characterization; refers to the broad and general process by which a material's structure and properties are probed and measured. It is a fundamental process in the field of materials science, without which no scientific understanding of materials could be ascertained.

The scope of the term often is very wide; here we will accept the broad definition of materials characterization which contains;

(1) Microscopic Characterization, (2) Spectroscopic Characterization, and (3) Macroscopic Characterization (Mechanical and Thermal properties).

The scale of the structures observed in materials characterization ranges from angstroms, such as in the imaging of individual atoms and chemical bonds, up to centimeters, such as in the imaging of coarse grain structures in metals.

While many characterization techniques have been practiced for centuries, such as basic optical microscopy, new techniques and methodologies are constantly emerging. In particular the advent of the Electron Microscope and X-Ray Characterization in the twentieth century has revolutionized the field, allowing the imaging and characterizing of micro structures and compositions on much smaller scales than was previously possible, that lead to a huge increase in the level of understanding why different materials show different properties and behaviors.

The broad definition of materials characterization contains:

I) Microscopic Characterization (Examination)

Microscopy is a category of characterization techniques which probe and map the surface and sub -surface structure of a material.
These techniques can use photons, laser, electrons, ions or physical cantilever probes to gather data about a sample's structure on a range of length scale.

II) Spectroscopic Characterization (Analysis)

These groups of techniques use a range of principles to reveal the chemical composition, composition variation, crystal structure and photoelectric properties of materials.

III) Macroscopic Characterization

(Mechanical and Thermal properties)
Material sampling sought to be representative of the structures studied, despite the limited number that could be collected further to Egyptian Ministry of Antiquities protocols on removal of materials from archaeological sites. The rock materials in the three heritage sites in Alexandria also sampled. Dimensions of the collected samples were reaching to 5*10*4 cm.

Sample labels, types, locations and construction periods are summarized in Table 2.

The collected Calcarenitic rock samples were analyzed by several analytical techniques. Thin sections partially dyed with alizarin red for readier identification of the carbonated phases, in particular the calcites and dolomites, were prepared for the petrographic analyses,

Table 1 Succession of beds in the coastal ridge of Alexandria

Recent deposits (2)	**Alluvial deposits (b)**	**Calcareous silt. Brown to buff. friable**
	Weathered oolites	**Weathered loose oolites**
Pleistocene deposits (1)	Upper member (b)	Thickness 2.0 to 7.5 ms. Oolitic intraclastic limestone. Yellowish white upwards becomes brownish yellow downwards. Fine to coarse grained. Friable with spherical algal flora and pumice
	Basal member (a)	Thickness 4.5 m. Skeletal sandy argilletic limestone. Brownish in color. Friable

and conducted on a JENAPOL polarising optical microscope (POM) fitted with a Canon 650 digital camera.

Samples of altered stone surface and core samples were taken in each of the studied monuments, according to their alteration degree, and to their height from the ground of structures, generally over the rising dump zone. A nonaltered sample of similar calcarenite was taken, for comparison with the altered stones of monuments.

To determine the physiochemical and physicomechanical behaviours of Calcarenitic rocks under study, intensive microscopic and macroscopic analysis were achieved by various analytic techniques such as:

A) Microscopic and Spectroscopic investigation

1 An X-ray diffractometer (XRD) PHILIPS PW-1730 (Cu K radiations), in the Laboratory of the civil engineering department of the University of Aristotle in Greece.

2 Thermal analyses DTA/TGA (for the collected rock samples).

3 X-ray fluorescence analysis (for the collected rock samples).

4 Chemical analyses (for plaster and painting layers collected samples).

5 An electronic microscope (SEM) model JEOL-JSM-840A, attached with EDX, X-Ray energy dispersive spectrometer unit (EPS oxford-Isis) was used in the General Service of Electronic Microscopy of geology department of the University of Aristotle in Greece.

6 Transmitted plane polarized light (for thin sections of the collected rock samples).

7 Study of the fabric of rock material (packing density and grain contact).

8 Stereoscopic observations (for the collected plaster and painting layers).

9 Porous media characterization. (Comparative study between the weathered and sound layers).

10 Pore size measurement and specific surface area by nitrogen BET-TPV.

11 Determination of the specific surface area (SSA).

12 Capillary water uptake measurements.

13 Saturation coefficient, S

14 Grain size characteristics of the weathered (salt contaminated) rock samples.

15 Geochemical/hydro chemical conditions in the sites included in this study.

I) Determination of Anions by Dioxen Ion chromatography (for the construction materials).

II) Atomic absorption spectrophotometer, determination of soluble cations and anions in the collected ground /underground water samples.

III) Suspension PH and conductivity.

B) Laboratory Geotechnical investigation (Mechanical Testing)

Table 2 Rock samples description

Type of rock	Site	Code	Dimensions	Location/Structure	Historic period
Intact Calcarenite rock (pure limestone)	Moustafa Kamil necropolis	M_1 M_2 M_3 M_4 M_5	The collected samples were reaching to 5*8*3 cm	Tomb 1 Tomb 1 Tomb 1 Tomb 2 Tomb 2	3rd to the first centuries AD
Sandy oolitic limestone	Catacomb of Kom El-Shoqafa	COM_1 COM_2 COM_3 COM_4 COM_5	The collected samples were reaching to 6*10*4 cm	2nd Floor 2nd Floor 3rd Floor 3rd Floor Main Well	2nd to fourth century AD
Oolitic intraclastic limestone	El-Shatbi necropolis	SH_1 SH_2 SH_3 SH_4 SH_5	The collected samples were reaching to 7*10*3 cm	Eastern Lucli Eastern Lucli Eastern Lucli Western Lucli Western Lucli	280 BC

Table 3 Evaluation Petrophysical and Geotechnical Evaluation Methodology which had been followed

Serial	Analytical procedure	Parameters
(I)	Material description–petrography	Geochemical composition
(II)	I) mineralogical analyses	Mineral composition
(III)	X-ray diffraction technique (for the collected rock and plaster and painting	Chemical compounds,
(IV)	layers)	Elemental composition,
(V)	Thermal analyses (for the collected rock samples)	Trace elements,
	X-ray fluorescence analysis (for the collected rock samples)	Soluble salts,
	Chemical analyses (for plaster and painting layers collected samples)	Anions/cations,
	II) Thin section analyses	PH-value,
	Transmitted plane polarized light (for the collected rock samples)	Organic compounds
	the fabric of rock material(grain contact /packing density)	Microtexture
	Scanning electron microscopy (SEM) observations, attached with EDX Micro-	Grain shape, grain size,
	probe (energy dispersive X-ray) microanalyses	Grain size distribution,
	Classes of weathering based on linear crack density and classification of the	Grain contacts, matrix/
	rock types included in this study	Ground mass/cements
	Stereoscopic observations (for the collected plaster and painting layers)	Recrystalization,intergrowth/
	Porous media characterization. (Comparative study between the weathered	Overgrowth, arrangement/
	and sound layers)	Orientation of components, inhomogeneities,anisotropies,
	Pore size measurement and Specific surface area by nitrogen BET-TPV	Interfaces, micro cracks,
	Determination of the specific surface area (SSA)	Micro morphology, roughness
	Capillary water uptake measurements	Porosity properties
	Saturation coefficient, S	Density, porosity, pore size, pore size distribution, pore surface
	Grain size characteristics of the weathered (salt contaminated) rock samples	Specific Surface area
	Geochemical /hydro chemical conditions in the sites included in this study	Hygric properties, hygroscopic capacity
	A) Determination of Anions by Dioxen Ion chromatography (for the construc-	Grain size distribution of rock/stones
	tion materials)	Geochemical hydro chemical composition
	B) Atomic absorption spectrophotometer, determination of soluble cations	Anions/cations
	and anions in the collected ground /underground water samples	Soluble salts, anions/cations
	c) suspension PH and electrical conductivity (EC)	PH value
	Geotechnical Investigation	Mechanical parameters
	A- Triaxial Compression Test	
	B- Brazilian strength (BTS)	

1 Triaxial shear test, determining the triaxial compressive strength and shear strength parameters (c) and (ϕ) of Clcarenitic rock types.

2 Brazilian splitting tensile strength (σ_t).

In this study, Table 3 summarizes the Petrophysical and Geotechnical evaluation methodology which had been followed.

Results and discussions of the microscopic and spectroscopic characterization and alanysis

Figure 2 represents the present geo-environmental conditions inside the archaeological sites under investigation; (a) Catacombs of Kom El-Shoqafa, after dewatering project and excavation of the third level of the Catacombs, photos taken in January 24, 2023. (b) El-Shatby Necropolis before and after the preservationand rehabilitation project, March 2023. (c) Moustafa Kamil tombs 1 and 2. The weathering process of Calcarenitic rocks at Alexandria monuments are linked to the textural characteristics; the bad geotechnical properties, the chemical carbonated composition of the Calcarenite, and the presence of soluble salts in the porous system. The marine climate, with characteristic flash flooding, heavy rain, humidity and marine sprays, are the important local factors contributing to the Calcarenite disintegration and degradation. Some decay forms such as honey comb weathering, stone bleeding and disintegration, contour scaling, biogenic crusts, red patinas, and alveolization are reported, as shown in Fig. 2. The factors and process of alteration must be studied in order to provide specific techniques of prevention, restoration, and optimal use of Calcarenite, which is still widely used in the region as ornamental stone for the buildings. The sulfates and chlorides affected the rock material by solution, migration, and salt weathering crystallization, hydration and thermal expansion mechanisms. Their origin is linked to the natural chemical weathering process of the rock in contact with atmospheric agents enriched by pollutants and marine products. The state of the surface below the crust is altered, and the weathering process seems to be active in this interface inducing more damage. The role played by the atmospheric pollutant sulfur dioxide is evident, where Sulphur dioxide is the pollutant gas most commonly found in the atmosphere and is usually present in high

Fig. 2 The archaeological sites under investigation. **a** Catacombs of Kom El-Shoqafa, after dewatering project and excavation of the third level of the Catacombs, photos taken in January 24, 2023. **b**. El-Shatby Necropolis, **c**. Moustafa Kamel tombs 1 and 2

concentrations in urban and industrial locations like Alexandria. It has led to intense weathering of these monuments in only some decades, in agreement with the fast growing of the traffic in Alexandria.

For detailed petrographic study of the Calcarenitic rock materials and fresco wall painting layers, Stereomicroscope, scanning electron microscope SEM, Thin sections analysis, X-ray diffraction, X-ray florescence analysis, thermal analyses DTA –TGA, pore media characterization analysis, grain size analysis and chemical analysis techniques have been carried out and the results are presented as follow:

X-ray diffraction analysis

X-Ray diffraction analysis (XRD) is a nondestructive technique that provides detailed information about the crystallographic structure, chemical composition, and physical properties of a material. From the X-ray diffraction XRD technique, it can be noticed that, the Catacomb of Kom El-Shoqafa is carved in the fossiliferous sandy Oolitic limestone (cemented sand); it is yellowish white massive fine to medium grained cross-bedded sandstone cemented with Calcareous cement. The construction material, (rock), characterized as Fossiliferous sandy Oolitic limestone is composed of Calcite $CaCO_3$ (47%),

Quartz SiO_2 (31%), Halite NaCl (12%), Gypsum $CaSO_4$. $2H_2O$ (10%).

It can be noticed from the XRD analysis, that the plaster layers which cover the walls of carakala hall in this catacomb, composed of three layers, lime (Calcite $CaCO_3$ layer with high percentage of fine rounded sand (Quartz SiO_2), covered with pure lime layer, covered with a white painting layer at the external surface as a base white painting layer which is painted with the pigments without medium, since these pigments interact with the wet calcium hydroxide layer and after that this layer dry and convert to Calcite $CaCo_3$ and fixed these pigments (real fresco). The black hard crust on the outer surface is a salty hard crust as a result of salt weathering. The components of these layers are Calcite 71%, Quartz 19%, Halite 8%, and Gypsum 2%.

Table 4 represents the Mineralogy of the three rock types under investigation. Table 5 summarizes the Average composition of the minerals for the represented plaster and painting layers samples.

And for the fresco painting layers (base white layer with a white painting layer) that these layers composed mainly of the Calcite $CaCO_3$ (70%), Quartz SiO_2 (22%), and contaminated with Halite NaCl (8%).

In El-Shatby Necropolis, the tombs are carved in fossiliferous oolitic limestone (conglomeratic in some parts), appearing sandy, due probably to weathering; the weathering phenomena are quite obvious starting at the surface and continuing inward, presenting big holes. The superficial shape of samples collected from the surround area, without presenting so intensity weathering phenomena, can be characterized also as granular but similar to a compact quartzite, the material is coloured yellowish because of the activity iron oxide solutions. The mineral composition is Calcite $CaCO_3$ 53%, Quartz SiO_2 25%, Hematite 11%, Gypsum $CaSO_4$. $2H_2O$ 11%, and some Cristobalite. The material can be characterized as medium—grained with uniform relative grain size; the grain shape is sub angular presenting equidimensional form and rough surface texture.

For the plaster layers which cover the most structural elements of this tomb, it is observed that these layers compose of three layers; the main intermediate layer contains of lime (Calcite $CaCO_3$) and sand (Quartz SiO_2), and this layer covered with good connected and strong gypsum layer as we notice from the analysis of cross section of these layers which gave the components of these layers Calcite 39%, Gypsum $CaSO_4$. $2H_2O$ 32%, quartz SiO_2 21% and Halite NaCl 8% as a result of salt weathering. The analysis of the main intermediate layer gave Calcite $CaCO_3$ 53%, Gypsum $CaSO_4$. $2H_2O$ 23%, Quartz SiO_2 14% and Halite NaCL 10% since this layer composed of lime and gypsum and quartz and weathered by salt weathering especially Halite NaCl.

In Moustafa Kamil tombs, the rock which are carved in the tomb 1 and 2 is fossiliferous sandy limestone, the material is composed of Calcite 52%, Quartz 28%, Gypsum 6%, Halite 12%, Hematite Fe_2O_3 2%. The rock is of white colour and can be characterized as medium grained with uniform relative grain size, angular to sub angular grain shape with equimensional form and rough surface texture. Sound pieces of rock are medium durables. Generally, the mineralogical composition of the bedrock of Moustafa Kamil tombs is mainly Calcite and Quartz with some Halite, Gypsum in addition to some iron oxides (Hematite). The rock material is severely weathered and presenting a sandy surface probably due to the different resistance of the grains to weathering processes. In many cases it displays a high porosity. The rock walls surfaces are not covered by crystal of Gypsum as it happen in Catacombs of Kom El-Shoqafa.

The main components of the renders and painting layers which covering the burial niches of these tombs are Calcite $CaCO_3$ (54%), Quartz SiO_2 (26%), Gypsum $CaSO_4$. $2H_2O$ (5%), and Halite NaCl (15%). The presence of Gypsum may be as trace component of the plaster layers and the red painting layer is compose of Hematite Fe_2O_3.

Thermal analysis (TGA/DTA)

From the thermal analysis (DTA, TGA), it is noticed that, % W.T of $CaCO_3$ for the collected rock samples from Catacombs of Kom El-Shoqafa is 64. 25. For the % W.T of free water is 0. 54 and for the % W.T of $Ca(OH)_2$ is zero for all collected samples.

Table 6 represents the results of DTA-TGA analysis for collected rock samples from the three archaeological sites under investigation.

Table 4 Mineralogy of the three rock types under investigation

Rock type	Calcite $CaCO_3$%	Quartz SiO_2%	Gypsum $CaSO_4.2H_2O$%	Halite NaCl%	Other
Fossiliferous sandy oolitic limestone (kom El-Shoqafa). (COM)	47–65	31–23	10–5	12–9	2
Intact Calcarenite (Moustafa kamil), (M)	52–72	28–18	8–3	12–6	3–5
Fossiliferous Calcarenite (El-Shatbi tomb, (SH)	53–80	25–20	11–7	11–7	3

Table 5 Average composition of the minerals for the representive plaster and painting layers samples

Plaster & painting layers	Calcite $CaCO_3$%	Quartz SiO_2%	Gypsum $CaSO_4.2H_2O$%	Halite NaCl %	Other
Catacomb of kom El-shoqafa, (Plaster layers)	71	19	2	8	2–3
Catacomb of kom El-shoqafa, (Plaster layers + white painting layer)	69	23	–	8	1
Moustafa kamil tomb (Plaster + red painting layer) M1	58	33	–	9	4–2
Moustafa kamil tomb (Plaster layers)M2	54	26	5	15	3
El-shatby tomb (Plaster layers) SH29	39	21	32	8	2
El-shatby tomb (Plaster layers) SH30	53	14	23	10	1–2

From the thermal analysis (DTA, TGA), it is noticed that, % W.T of $CaCO_3$ for the collected rock from El-Shatby necropolis is 87. 91. For the % W.T of free water is zero. For the % W.T $Ca(OH)_2$ the results are zero for all collected rock samples.

It is noticed from thermal analysis (DTA-TGA), that % W.T of $CaCO_3$ for the collected rock samples from Mustafa Kamil tombs is 89. 61. For the % W.T of free water is zero. The % W.T of $Ca(OH)_2$ is zero for all collected samples.

X-ray fluorescence (XRF) analysis

The results from the X–Ray Florescence (XRF) technique refered to the elemental arrangement for the rock samples collected from Catacomb of Kom El-Shoqafa which can be put in a decreasing order according to their concentration as follow:

(Sample COM1); CaO (51.54%), SiO_2 (14.55%), MgO (1.07%), Al_2O_3 (2.51%), SO_3 (0.59%), Fe_2O_3 (1.05%), Na_2O (0.15%), K_2O (0.02%), TiO_2 (0.04%), P_2O_5 (0.03%) and L.O.I (28.20%). The total is (99.75%).

It can be noticed from the instrumental chemical analysis that, the dominant constitute of the render layers which cover the most walls of Carakala hall in Catacomb of Kom El-Shoqafa is lime CaO with high percentage of coarse and fine free sand SiO_2 of natural origin.

For the fresco painting layers (Sample COM2), it is noticed that it constitutes of lime CaO layers. The white painting layer in the external surfaces is lime CaO and the aggregates are natural sand SiO_2.

Petrography examination of rock samples (thin section analysis)

From the thin section examination (transmitted plane polarized light) for rock samples collected from Catacombs of Kom El-Shoqafa, it was noticed that in the internal structure of the rock body we can observe the dominant components, which are bioclasts of gastropods, foraminifera, algae, and shell debris. The most of them are with test wall of neomorphic microspar, while the tests are internally filled with micrite and microspar. Surrounded monocrystalline Quartz grains are detected and are of variable size and iron oxides contours marking the previous existence of K-feldspar grains. Ooids and peloids are also composing this fossiliferous sandy oolitic limestone, or cemented sand, as shown in Fig. 3.

The petrographic (thin section) study of El-Shatby tombs has been carried out on five rock samples [Code Nr (SH)], which collected through a vertical profile taken through these tombs. The limestone of El-Shatby tombs can be classified into two texture types, namely packstone and wackestone. These two texture types are with different percentages of quartz grains, bioclasts, Ooids, and peloids. Such texture type of limestone indicates that it is deposited in shallow agitated marine environment

Table 6 Results of DTA-TGA analysis for collected rock samples from the three archaeological sites under investigation

SampleCode	Site	Rock type	% W.T. Free water (H_2O)	% W.T. $Ca(OH)_2$	% W.T. $CaCO_3$
(M)	Mustafa kamil tombs	Intact calcarenite	–	–	89.61
(COM)	Catacomb of kom El-shoqafa	Fossiliferous sandy oolitic limestone	0.54	–	64.25
(SH)	El- shatbi tombs	Fossiliferous Calcarenite	–	–	87.91

forming oolitic grains associated with detrital quartz grains, and few grains of microcline. Most of the Ooides composing this limestone lack their internal structure and this is usually a result of micritization by endolithic algae the algal debris in the studied thin sections which ensure the reason of Ooids micritization. The rock porosity types in the studied thin sections are of intergranular and intragranular type, as shown in Fig. 4.

The rock texture at Mustafa Kamil tombs is of two textures, namely packstone and wackestone. These two texture types show different percentages and sizes of Quartz grains and different bioclasts especially foraminifer's tests. Most of the Ooides have lost their internal structure, while few of them retain their internal concentric structure. Porosity has been greatly reduced as noted due to filling with drusy sparite. The cementation of the components of this limestone is represented by isopachous microspar, as shown in Fig. 5.

Scanning electron microscopy attached with energy dispersive X-ray spectroscopy (SEM/EDX)

Significant data can be obtained from the Scanning Electron Microscope (SEM) images and EDX micro analysis. SEM observations on the collected rock samples from Catacomb of Kom El-Shoqafa show the main components of this rock which contain the monocrystalline quartz grains, iron oxides contours marking, shell debris, in adition to Ooides and peloids which are also composing this Calcarenitic rock. The porosity of this rock is about 20% of the thin section. Numerous small patches of salts crystals are obvious on the rupture surface, which may explain the great reduction of Uniaxial Compressive Strength σ_c and Young's modulus of this rock samples.

The original eolian sediment was formed as an alternate sequence of thin fine and medium sandy layers due to cyclic time variation of the transport agent competency. It is interesting to note that the fine sand layers appear to show a less porous arrangement of grains and iron oxides. This observation suggests that it may have a lower hydraulic conductivity. The observed greater concentration of iron oxides in this rock layers could result from water retention by capillary action, which is the condition that favours the precipitation of iron oxides. Because of the better drainage, weathering processes could act more intensively in the medium sandy layers. For these layers, the number of contacts between grains is clearly much smaller in compression with the fine sandy layers. Such contacts are essentially punctual, while tangential contacts are seen in the fine sandy layers.

The degrees of the collected weathered rock samples summarized in Table 7.

For the plaster and fresco painting layers which cover the structural elements of the Catacomb of Kom EL-Shoqafa and decorate the burial niches, it is observed in the cross-section of the samples that, The dominant constitute of these layers is Calcite grains with fine Quartz grains. The external white painting layer consist of Calcite, and the internal layer with high content of Quartz grains, no cracks, no fibres observed. There is a distinct compaction zone at the surface where the pore space is completely filled with salts. The thickness of this zone is obviously influenced by the condition of the material pore space.

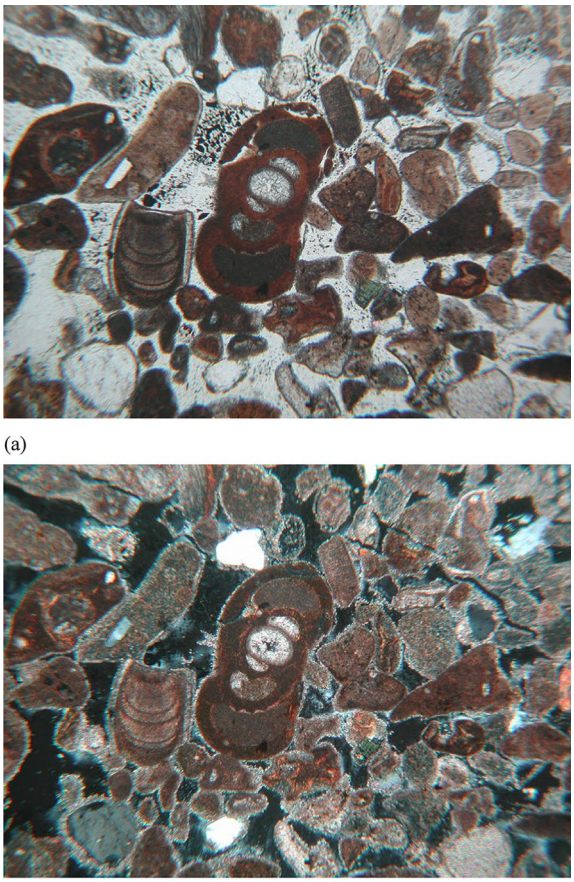

(a)

(b)

Fig. 3 Photomicrograph of fossiliferous sandy oolitic limestone, (**a**)under parallel polarized light. (**b**) under cross polarized light (XPL), showing bioclasts of gastropods, foraminifera,algae,and shell debris,most of them are with test wall of neomorphic microspar, filled with micrite and microspar, Catacomb of Kom El-Shoqafa (Weathered sample, cracks between and through the minerals).

EDX micro analysis shows that in some cases, the weathering layers are enriched in Ca, C, O, Si, Na, Cl, S, K and Mg.

The cementation of the limestone components of El-Shatby tombs is represented by cementation by isopachous microspar that is also noticed in scanning electron microscope images. This indicates that cementation took place in a phreatic zone some pores

(a) Unweathered sample.

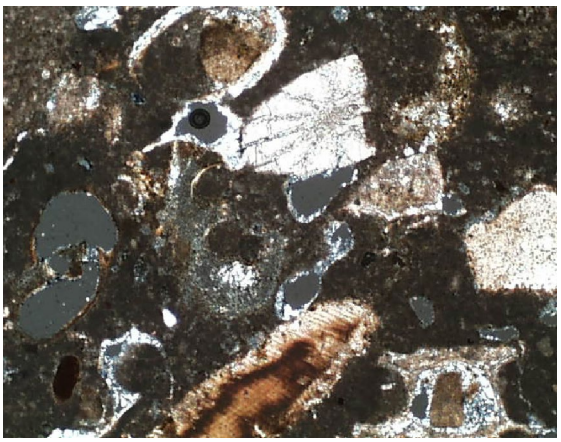

(b) Unweathered sample.

Fig. 4 **a**, **b** Photomicrograph of fossiliferous Calcarenite rock thin section under cross polarized light (XPL)showing detrial quartz grains, bioclasts, Ooides, peloids, algal debris and porous region, El-Shatby Necropolis

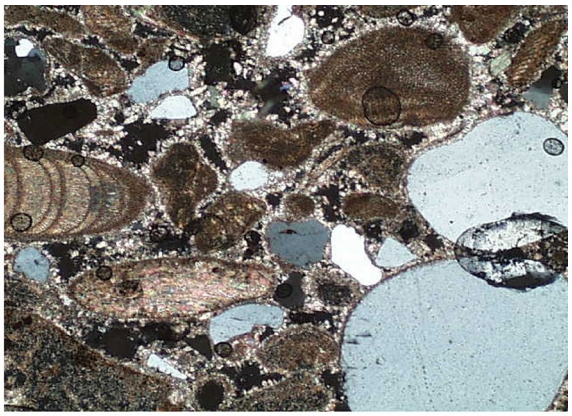

(a)

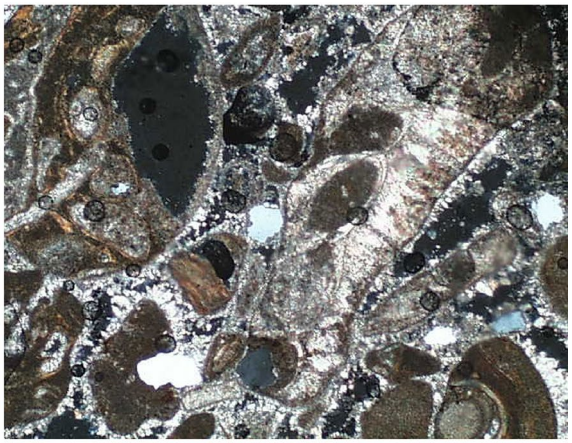

(b)

Fig. 5 **a**, **b** Photomicrograph of intact Calcarenite under cross polarized light (XPL) showing wackestone texture with drusy sparite, shells, and detrial grain sand Moustafa Kamil tombs 1 and 2. (unweathered sample)

are filled with drusy sparite which is a meteoric cement type and such cement is an indication of meteoric phreatic environment.

EDX analysis shows that in some cases, the weathering rock layers are enriched in Ca, C, O, Na, Cl, S, Si, Mg, and K.

For the plaster layers which cover the most structural elements of these tombs, it is observed from the examination of the cross-sections that these layers consist of three compacted layers. The second layer of 1 cm thickness contains of Calcite and few Quartz grains and in contact with a 3 mm thick outer Gypsum layer. There is a strong contact with another mortar with high percentage of coarse Guartz grains and pieces of crushed brick. There are crystalline salts in the internal structure of the samples.

For the plaster sample code Nr (SH 3), high percentage of fine sand with light in colour well observed. There are rounded sand and glass like broken particles in the main layer which contains lime and gypsum. There is black deposited on the external surface and white layer of 0.5 cm thickness. There are recrystallization phases as secondary phases. There are also few small pores, but no fibers, no enclosures. The compaction of layers is medium.

The elemental arrangement for the rock samples collected from El-Shatby tombs can be put in a decreasing order according to their concentration as follow:

(SH1); CaO (53.81%), SiO_2 (4.54%), MgO (1.07%), SO_3 (0.2%), Al_2O_3 (0.63%), Fe_2O_3 (0.4%), Na_2O (0.14%), K_2O (0.03%), TiO_2 (0.04%), P_2O_5 (0.05%) and L.O.I (38.83%). The total is (99.74%).

SEM observations on the collected rock samples from Moustafa Kamil tombs show increase of the porosity of various sizes has been greatly reduced as noted due to filling with drusy sparite. There are different percentages and sizes of Quartz grains and Ooides. At some places

Table 7 Definition of the degree of weathering

Grade	Term	Typical characteristics
(I)	**Unweathered**	Unchanged from original state, no evident micro fracturing, and slight discolouration on major discontinuity surface
(II)	**Slightly weathered**	Slightly discolouration,slight weathering, weathering penetrates through most discontinuity surface
(III)	**Moderate weathered**	Considerably weakened, penetrative discolouration, large pieces cannot break by hand
(IV)	**Weathered**	Significantly weaken than the fresh rock. easily breakable with hand
(V)	**Completely weathered**	Original texture is present, all microfractures tend to be open, losses most of strength of fresh rock
(VI)	**Residual weathered**	Soil derived by in situ weathering but retaining none of original texture or fabric

there are micro cracks at the minerals contacts or even inside of minerals. Microscopic examinations show a very inhomogeneous distribution of salt crystals along the sample cross-section. The observations indicate that, the occurrence of geometrical shapes are not related to the structure.

EDX micro analysis showed that in some cases, the weathering layers are enriched in Ca, C, O, Si, Na, Cl, S, K, Mg, and Al.

From the examination of the cross-sections of the plaster and painting layers which decorate the burial niches of Moustafa Kamil tombs, it is observed that, these layers consist of Calcite with high percentage of fine rounded Quartz. Some pieces of a glass like material observed, also many cracks are noticed through the samples. There are Calcite lumps, inhomogeneous distribution of salts inside the structure of the sample.

Water soluble salts (Halite and glauberite) have been observed on the top of the weathered layers in forms of needles crystals.

EDX micro analysis showed that in some cases, the weathering layers are enriched in Ca, C, O, Si, Na, Cl, S, Mg, and K.

The elemental arrangement for the rock samples collected from Moustafa Kamil tombs can be put in a decreasing order according to their concentration as follow:

(M); CaO (50.45%), SiO_2 (11.94%), MgO (1.12%), Al_2O_3 (0.93%), SO_3 (0.27%), Fe_2O_3 (0.5%), Na_2O (0.35%), K_2O (0.04%), TiO_2 (0.09%), P_2O_5 (0.01%) and L.O.I (34.07%). The total is (99.77%).

Stereoscopic observation system (SOS)

The Stereoscopic observations for collected plaster and fresco painting layers samples from Catacomb of Kom El-Shoqafa code Nr (COM1) showed that, the dominant constitutes of the plaster layers which cover the most walls of Carakala Hall is lime with fine rounded sand of natural origin with light-colored in medium proportion. Black hard crust on the outer surface cover the white painting layer is obvious, with internal contact with a more brownish layer with high content of sand. since these plaster layers contains of three connected layers. No cracks observed. The thickness of this layer is 0.5 mm with white colour. Pores are negligible, no fibers and enclosures. The layers are very compact.

For the fresco painting layers sample Nr (COM2), it is observed that, 0.5–1 cm fine, white in colour lime layers in contact with a 4 mm of white painting layer in the external surface ($CaCO_3$). The contact is good. The aggregates are natural sand with sieze 0.2 mmwith light color in medium –high percentage. Small pores of mean diameter 400–600 μm in 5% percentage are obvious. There are no fibers nor enclosures, and the compact of the sample is medium.

From the stereoscopic examination which carried on the collected plaster and fresco painting layer samples from Moustafa Kamil tombs, it is observed that, for the sample Nr (M1), the plaster which cover the walls of tomb (1) contains lime layer with high percentage of fine rounded sand, light in colour, also some pieces of a glass –like material are participating as aggregates. Very strongly compacted and good contact between aggregates and binders are observed. Small pores of mean diameter d = 300 μm to a high percentage 10% and layer pores of d = 1 mm in low percentage 1–3% were noticed. For the salts, crystalline salts in form of needles in the samples were noticed with no cracks, for the enclosures, lime lumps, shells inside the structure were noticed. And the sample is very compacted with pinkish white color.

The observations of the sample Nr (M2) showed that, the fresco painting layers which decorate the burial niches of these tombs contains lime with fine aggregates of 500 μm diameter and have a glassy form. The aggregates are rounded and light red in colour with 3 mm thickness. The red painting layer in the external surface is hematite (Fe_2O_3) mainly. There are few pores of diameter

100 μm. For the enclosures lime lumps well observed. The compact of layers is medium, and the colour is pinkish white.

Surface area analyzer (BELSORP). Porous media characterization (micro porosity, TPV and BET)

In order to characterize the porous media of the Calcarenitic rock samples from the weathered and unweathered layers coolected from the same sites under investigation. The nitrogen absorption technique, capillary imbibition techniques, and the specific surface area determination (SSA) were used.

This technique is using liquid Nitrogen to determine the surface area of any material, especially, the Nano-Catalysis substances. This technique is very important for many research sectors. Specifications of this technique include: Up to 6 samples per run.

Nitrogen as adsorption gas. 400 °C maximum pretreatment temperature 0.0.01 m^2/g and more as a measurable specific surface area range.

From the porous media characterization study on the collected rock samples from weathered layers collected from Catacomb of Kom El-Shoqafa (COM1), it is noticed that the pore diameter distribution of these rock samples is 10–20A (4%), 20–30A (9.17%), 30–50A (11.1%), 50–100A (15.847%), 100–200A (17.80%), and 200–1960 A (41.97%). Nm is 2.26599 E-05, and BET (m^2/gr) is 2.21098, and TPV (ml/gr) is 0.00992. Micro porosity % is 1.79327, as shown in Figs. 6 and 7.

But the rock sample which collected from the unweathered (sound) layers from the same site (COM2) it is noticed that: the pore diameter distribution of this rock is 10–20A (9.46%), 20–30A (12.5%), 30–50A (14.98%), 50–100A (12.72%), 100–200A (7.93%), 200–2040A (42.4%), and nm 1.5522E-05, BET(m^2/gr) 1.51452, TPV (ml/gr) 0.00232, and micro porosity % is 0.42542, as shown in Figs. 8 and 9.

The mean specific surface value for the collected weathered rock samples from Catacombs of Kom El-Shoqafa is 1.9 m^2/g and 1.7 m^2/g for the unweathered (sound) samples.

It can be noticed from the pore size distribution analyses that, the pore diameter distribution of the rock samples collected from the weathered layers from El-Shatby necropolis (SH31) is 10–20A (4.65%), 20–30A (3.03%), 30–50A (4.15%), 50–100A (4.4%), 100–200A (4.1%), and 200–2044 A (79.71%). nm is 2.44596E-05, BET(m^2/gr) is 2.38659, TPV (ml/gr) is 0.01472 and micro porosity % is 2.98523. The Adsorption/desorption isotherm diagram and pore media distribution of the weathered layers are shown in Figs. 10 and 11.

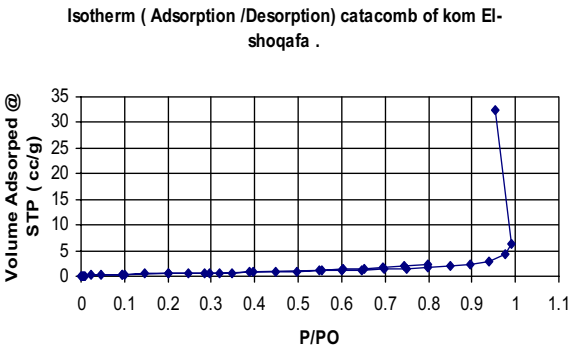

Fig. 6 Adsorption/desorption isotherm for weathered rock sample collected from Catacomb of Kom El-Shoqafa (COM_1)

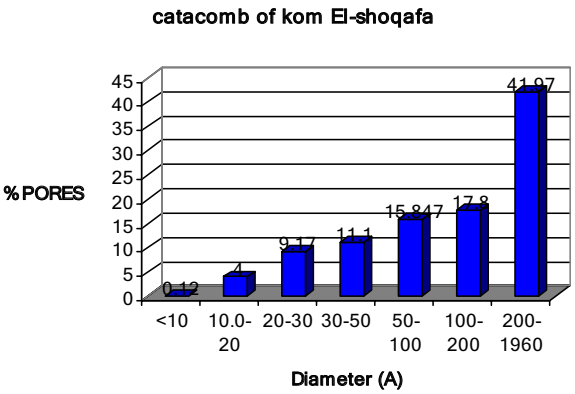

Fig. 7 Pore size (diameter A) distribution for collected weathered rock sample from Catacomb of Kom El-Shoqafa (COM_1)

But for the collected rock samples from unweathered (sound) layers collected from the same site (SH2), it is noticed that the pore diameter distribution of these rock samples is 10–20A (5.77%), 20–30A (4.04%), 30–50A (5.07%), 50–100A (5.67%), 100–200A (4.00%), and 200–1950 A (74.56%). nm is 2.52529 E-05, and BET(m^2/gr) is 2.46399, TPV (ml/gr) is 0.01186, and micro porosity % is 2.41793, and for the Adsorption/desorption isotherm diagram and pore media distribution of the unweathered layers shown in Figs. 12 and 13.

The specific surface are for the collected weathered rock samples from El-Shatby necropolis are 1.5 m^2/g and 1.3 m^2/g for the unweathered samples.

For the rock sample were collected from the weathered layers from Moustafa Kamil tombs (M1), it is notice that, the pore diameter distribution of this rock is 10–20A (0.05%), 20–30A(0.036%), 30–50A(0.05%), 50–100A(0.054%), 100–200A (0.045%), and 200–2330A (99.76%). nm is 2.86707E-05, BET (m^2/gr) is 2.79748,

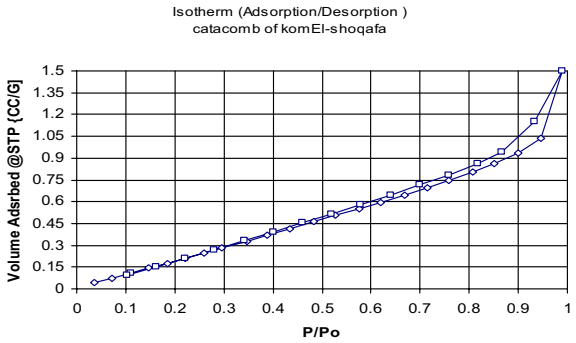

Fig. 8 Adsorption /desorption isotherm for unweathered rock sample collected from Catacomb of Kom El-Shoqafa (COM_2)

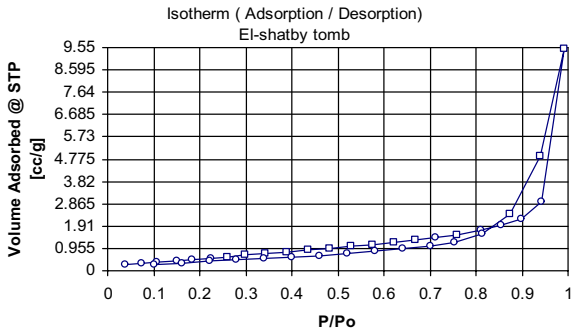

Fig. 10 Adsorption/desorption isotherm for weathered rock sample collected from El-Shatby tombs (SH_31)

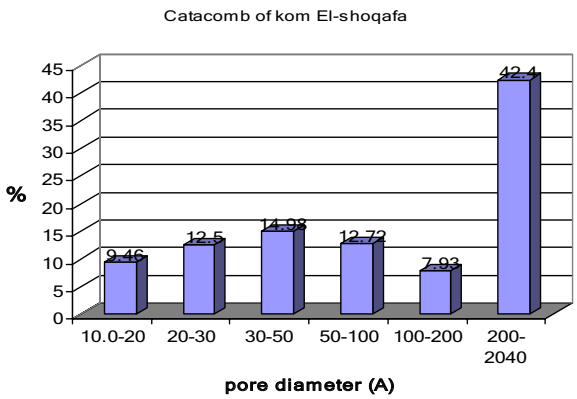

Fig. 9 Pore size (diameter A) distribution for collected unweathered rock sample from Catacomb of Kom El-Shoqafa (COM_2)

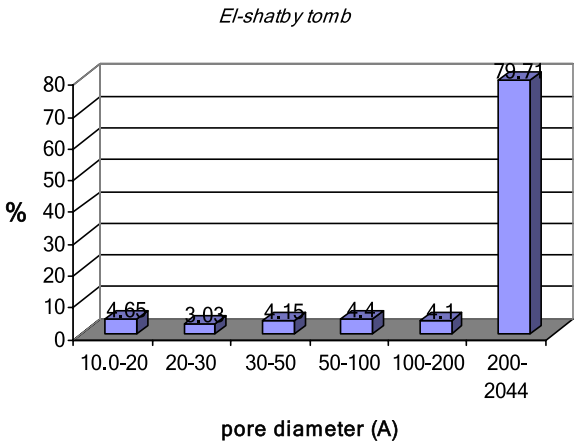

Fig. 11 Pore size (diameter A) distribution for collected weathered rock sample from El-Shatby tombs (SH_31)

TPV (ml/gr) is 1.48453, and micro porosity % is 74.32496. The Adsorption/desorption isotherm diagram and pore media distribution of the weathered layers shown in Figs. 14 and 15.

But for the collected rock samples from unweathered (sound) layers collected from the same site, it is noticed that the pore diameter distribution of these rock samples is 10–20A (7.667%), 20–50A (11.065%), 50–100A (7.667%), 100–200A (6.956%), and 200–1996 A (65.34%). nm is 2.21145E-05, and BET(m^2/gr) is 2.15777, TPV (ml/gr) is 0.00749, and micro porosity % is 1.43966. the Adsorption/desorption isotherm diagram and pore media distribution of the unweathered layers are shown in Figs. 16 and 17.

The mean specific surface area is 1.4 m^2/g for the collected weathered rock samples, and 1.3 m^2/g for the unweathered rock samples.

For the capillary water uptake the mean value for the collected rock samples from the unweathered layers from collected rock sample is 2.1 kg/m^2 $h^{0.5}$.

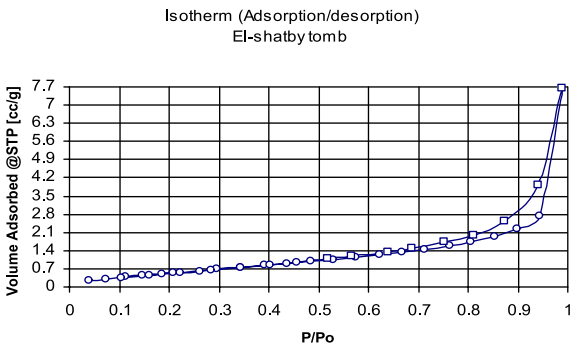

Fig. 12 Adsorption/desorption isotherm for unweathered rock sample collected from El-Shatby tombs (SH_2)

Wet chemical analysis

From the chemical analysis which have been carried on two collected plaster samples, it is noticed that the plaster layers which cover the structure elements of El-Shatby necropolis are constitute of lime (CaO) layers,

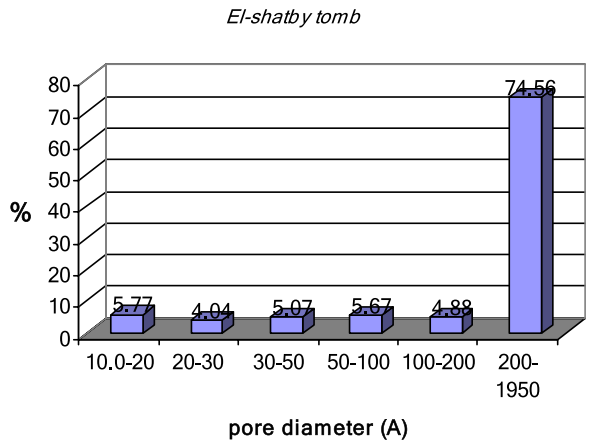

Fig. 13 Pore size (diameter A) distribution for collected unweathered rock sample from El-Shatby tombs (SH_2)

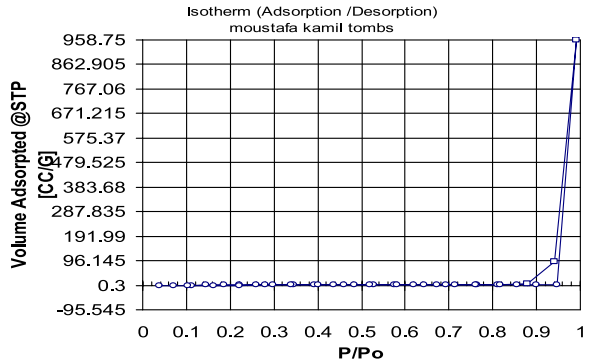

Fig. 14 Adsorption/desorption isotherm for weathered rock sample collected from Moustafa kamil tombs (M_1)

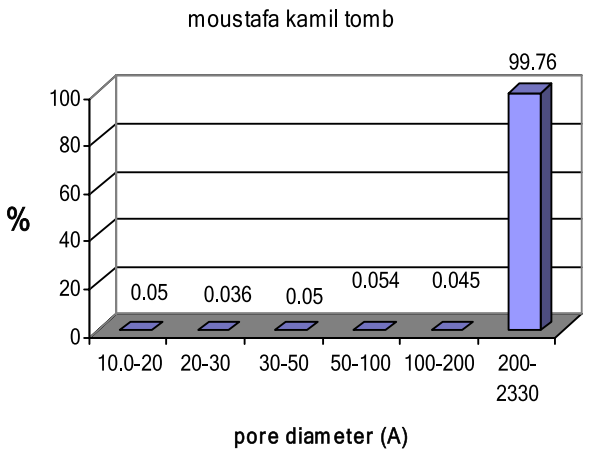

Fig. 15 Pore size (diameter A) distribution for collected weathered rock sample from Moustafa Kamil tombs (M_1)

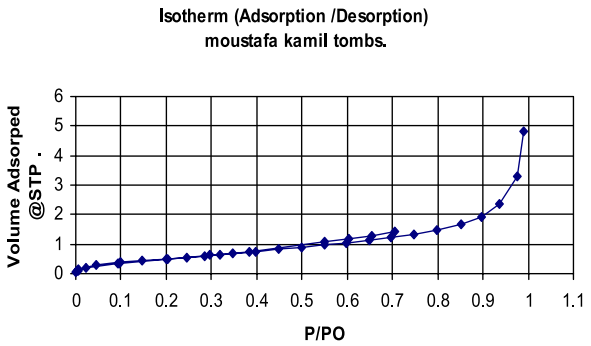

Fig. 16 Adsorption/desorption isotherm for unweathered rock sample collected from Moustafa Kamil tombs (M_2)

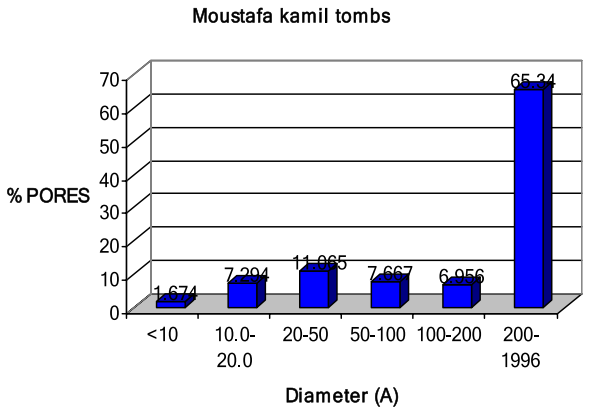

Fig. 17 Pore size (diameter A) distribution for collected unweathered rock sample from Moustafa Kamil tombs (M_2)

with high percentage of coarse sand ($SiO_{2)}$. Glass- like fine aggregates, crushed bricks and fine rounded sand are obvious. In the white layer there are no crushed bricks, only sand and glass-like aggregates. Also there are crystalline salts in the structure of the samples.

The Chemical analyses were carried out to determine the chemical composition of the studied plaster and fresco painting layer samples from these tombs.

For each sample, the composition in acids W.T % and the composition in soluble oxides in 0.1 NH CL as well as the content in water soluble salts was determined.

It is noticed from these results that, the plasters which cover the walls of Moustafa Kamil tombs (1, 2) code Nr (M1, M2) constitute of lime CaO layer with high percentage of sand SiO_2 and the fresco painting layers which decorate the burial niches of these tombs constitute of lime CaO with fine aggregates, and the red colour (painting layer) is iron oxide Fe_2O_3 hematite in the external surface.

Water uptake measurements

The Water uptake in the unweathered layers is higher than in the weathered layers, and this indicating a pore system which cannot transport water as quickly as in the sound unweathered layers. Most likely caused by a higher content of micro pores containing moisture and salts. The mean value for the collected Calcrenitic rock

samples from the weathered layers from Catacomb of Kom El-Shoqafa is 1.4 kg/m^2 $h^{0.5}$.

Grain size distribution (GSD). particle size and zeta potential analyzer, (Malvern Zetasizer Nano Series).

The device Malvern Zetasizer Nano Series is used to measure the particle size of any geomaterial that could be suspended in a solvent. The precision reaches the limit of 20 nm. This Technique uses the properties of the Laser Beam. Also this device can measure the potential of charged particles present in any medium.

Temperature control range from 0 laser 10 mW, 633 nm, Min sample volume 12 micro -liter, Zeta Potential Range: ± 500 mV.

For the Catacombs of Kom El-Shoqafa, the Grain size data show that considerable breakdown to the components of the rock has occurred, as there is no peak around 600 μm as one might expect if ooids were simply being released by weathering. It is also echoes the findings of various laboratory simulation studies of salt weathering effects on a wide range of rock types.

For Mustafa Kamil tombs, the grain size data show that considerable breakdown to the components of the rock has occurred, as there is no peak around 600 μm as one might expect if Ooids were simply being released by weathering.

Geochemical/Hydro chemical conditions

For the Geochemical/Hydro chemical conditions in Catacombs of Kom El-Shoqafa, it is noticed that all the plaster and Calcarenitic rock samples showed much higher salt contents and for the two plaster samples collected from Catacomb of Kom El-Shoqafa (2–2.5 km from the sea and very close to maruit lake 400 m) the values were 0.47 and 0.85% for chloride CL, and 1.64 and 1.56% for sulphate SO_4. The chloride contents were consistently higher than the sulphate content, and the mean difference for the six samples was 45.59 times. Quantitatively, therefore chloride is the dominant salt. And the analytical results for the rock collected samples were very close to the results which obtained from the analysis of the plaster samples.

For the geochemical/Hydro chemical conditions in El-Shatby Necropolis

It is found that, all the plaster and rock samples showed much higher salt contents. The greatest increase were for the two plaster samples from El-Shatby tomb (75 m from the sea) samples code Nr (SH 29, SH 30) their mean values were 5.66% and 5.07% for chloride CL, and 14.15 and 6.37% for Sulphates.

The chloride contents were consistently higher than the sulphate content, and the mean difference for the six samples was 45.59 times. Quantitatively, therefore, chloride is the dominant salt. The analytical results for the rock collected samples were very close to the results which obtained from the analysis of the plaster samples.

But El-Shatby water samples refer that, the water which are flooding or inundated all the ground of the tomb are sea water. Also it is notice that the dominant anions are the chlorides 2066–2056 ppm, followed by the sulphates which are 556–759 ppm. This refers that the dominant hypothetical dissolved salts in these water samples are chlorides Na Cl, and sulphates Na SO_4. As this site is close to the sea shoreline just 75 m, since the ground level of the tombs is under the sea level about 60–78 cm, and it is 6 mbelow the normal ground level (El-Corniche street).

For Moustafa Kamil tombs, there is no underground water on the ground level of the tombs (1) and (2), and the chemical analysis carried out on the rock and renderings samples.

The mean value of (EC) for the collected rock samples from Moustafa Kamil tombs is 0.638. While the mean value of PH value for the collected rock samples was 7. From the Geochemical/Hydro chemical conditions study in this site, it is noticed that all the plaster and rock samples showed much higher salt contents. For the two plaster samples from Moustafa Kamil tombs showed increase in chloride 1.26, 0.58% for chlorides, and 0.57%, 0.55% for sulphates, and 0.20% for Nitrates NO_3. The chloride contents were consistently higher than the sulphate content, and the mean difference for the six samples was 45.59 times. Nitrate salts have been detected only in the hydro chemical analysis for the examined rock samples collected from Moustafa Kamil tombs. This is due to four reasons, namely: carbonates are not good sink of nitrate, NO_2 is with very low concentration at study area. Nitrate salts are highly soluble and easy to be leashed from stone surface by rainfall [37, 38].

Atomic absorption spectrophotometry analysis (Shimadzu AA-7000)

Atomic Absorption (AA) occurs when a ground state atom absorbs energy in the form of light of a specific wavelength and is elevated to an excited state. The amount of light energy absorbed at this wavelength will increase as the number of atoms of the selected element in the light path increases. The relationship between the amount of light absorbed and the concentration of analyses present in known standards can be used to determine unknown sample concentrations by measuring the amount of light they absorb. This device has many applications in archaeology, heritage science, pharmacology, environmental studies, biophysics, and toxicology.

The advantages of this technique includes, double-Beam optics and stable hardware achieve superior stability. Very low limits of detection. Very advanced safety technology.

From the Atomic absorption spectrophotometry analysis results it can be noticed that the type of water in the Catacomb of Kom El-Shoqafa is stagnant water not sea water and this water is a result of seepage water from mariute lake, and it can notice that the dominant anions are the sulphates which are from 845 to 1156 ppm than the chloride which are 400–390 ppm, and this refer that the hypothetical dissolved salts are Sulphates mainly Na SO_4 and Na CO_3, followed by Chlorides mainly Na Cl.

Considering the observations on –site together with measurements of micro porosity, salt content and analyses of the pore structure by microscopy, nitrogen absorption techniques, capillary imbibitions techniques, and specific surface area determination, it is possible to explain the processes of weathering at the sites under investigation. The deterioration rises by cyclic salt crystallization of predominantly sodium chloride NaCL, and sodium sulphates Na_2SO_4 crystallizing in different hydrates which process is controlled by the ambient relative humidity. The weathering process is forced when the salts are concentrated in the back –weathered area and sheltered from rain-wash.

The weathering features as well as the laboratory analysis of the collected rock samples indicate a high impact of salt weathering on these archaeological underground structures on macro scale and grain scale. The rock texture type and composition (e.g. Sparitic or Micritic limestone, and microstructure) have been examined as they are highly controlling the rock durability in particular to salt weathering, wetting and drying associated with insulation solar) heating.

There are three possible salt sources to the built heritage in Alexandria, namely: sea spray, air pollution and sewage water. These sources are expected based on the field and laboratory data that has been collected and examined in this study.

In this marine environment, it is observed that the damage for the archaeological structures caused by salt accumulation requires a succession of transfers in liquid and gaseous phases. On the Calcrenitic rocks, the main degradation can be explained by the successive penetration of solutions from the ground, which migrated by capillarity, and then evaporated with halite precipitation. When the petrophysical properties allow fast and long-distance transfer and the porosity allows a flow that compensates evaporation, salts crystallize on the surface without causing significant weathering. In contrast, when the capillary supply does not compensate evaporation, salts precipitate inside the porous of stone, under the surface, where looseness of superficial crystals results.

The weathering of these types of Calcarenitic can be explained by its very weak porosity and its irregular capillary transfer. This degradation implies a successive supply of sea-spray droplets, and the evaporation and precipitation of the salts onto the stone's surfaces. These limestones contaminated by salts. At relative humidities 75%, the presence of water vapor until the salts dissolve ensures weak superficial penetration by capillary suction, the solution to evaporate and the halite to precipitate inside the pores and cracks underneath the superficial crystals. This weathering mechanism by fixation of water vapor is mostly hidden by liquid water transfer by capillarity. Rain, which supplies capillary transfer from the ground leaches the salts deposited on the surfaces of the stones.

In addition to the two methods of weathering already described, rain is a factor that also increases the Calcarenitic's deterioration and limits the limestone's degradation. In spite of the numerous factors that play a role in salt weathering, the evolution of only one factor can change the relative importance of weathering mechanisms. In this way, on the limestone and on the sandstone, these two mechanisms can act simultaneously, on their own, or alternately leading to the same forms of weathering.

The degradation caused by capillary transfer observed on these Ca;carenitic rocks corresponds to a well-known mechanism on nearly all buildings and in nearly all climates. In the field, this method of weathering can be limited, but not totally avoided, unless objects are placed inside buildings. However, the mechanism of water fixation until deliquescence of salts occurs on the stones, although less spectacular, is impossible to limit in the field without modification of the petrochemical properties of the stone products). On salt-contaminated stones placed in a museum, sheltered from precipitation, this mechanism can continue and only humidity control can limited it.

The most important mechanism for salt damage appears to be crystallization pressure. Nevertheless, although several theoretical models, extensive experimental and field data are reported in the literature, it is not yet clear what are the most important parameters which control the location and degree of damage. Few kinetic studies have been performed.

It appears that damage from salts is a complex series of processes resulting from the intricate interaction of different parameters, including the properties of the substrate, the solution and the salts, and environmental parameters. Kinetic factors, such as the crystal growth

and dissolution rate, also appear to play an important role.

Several articles on the distribution of salts in porous media in the field had been published. They point out the strong correlation between decay rates, the morphology of salt crystals, and the support moisture content, they observe that crystallization in the field is strongly influenced by relative humidity changes and for most salts to a lessee's extent by temperature modifications.

Salt crystallization is one of the most powerful weathering agents, especially when combined with wet/dry activity. In porous materials, crystallization pressure—which depends on pore structure, the saturation degree of salt and the energy difference between the crystal and the pore wall is the most important decay mechanism that occurs during salt weathering. It is well known that crystallization pressure is lower in larger pores and high saturation levels lead to high crystallization pressure. The energy difference between the crystal and the pore wall originates from surface forces. As a result, a substantial amount of energy is normally required to produce direct contact between salt and the material, setting the upper limit of crystallization pressure and, therefore, producing high levels of damage.

Table 8 Represents the fissuration index of the Calcarenitic rock types under investigation. Table. 9 Summarizes the types of primary and secondary porosity.

Table. 10 Summarizes the Micro porosity %, BET, TPV, nm, specific surface, water absorption coefficient W, saturation coefficient S, for the collected weathered/unweathered rock samples from the sites under investigation.

Results and discussions of the macroscopic analysis and mechanical testing

Triaxial shear test; determining the triaxial compressive strength and shear strength parameters of soft Calcrenitic rocks types

An isotropic Triaxial compression tests performed on an undistributed Calcarenitic rock samples collected from thethree archaeological sites. The specimen axis is perpendicular to the bedding planes. Significant results and findings from the from the Triaxial shear test obtained. For the Catacombs of Kom El-Shoqafa. Figure 18. represents the tress–strain curves in triaxial tests at various confining pressures. Failure envelope and strength parameters of sandy oolitic limestone, Mohr circles diagram from quick –undrained tests as shown in Fig 19. The results of undrained triaxial tests on sandy Oolitic limestone, principal stress ratio versus volumetric and axial strain are represented in Fig 20. The results of undrained triaxial tests on sandy oolitic limestone, volumetric strain versus axial strain are shown in Fig 21. For El-Shatby Necropolis. Figure 22. represents the tress–strain curves in triaxial tests at various confining pressures. Failure envelope and strength parameters of sandy oolitic limestone, Mohr circles diagram from quick –undrained tests as shown in Fig 23. For Moustafa Kamil Tombs, Fig 24. represents the tress–strain curves

Table 8 Fissuration index of the rock types under investigation

Rock type	Linear crack density (crack/mm)
Fossiliferous sandy oolitic limestone, catacomb of kom El-shoqafa (COM)	1.9 3.3 1.4
Intact Calcarenite,El-shatbi tombs (SH)	3.6 5.9 4.3
Intact Calcarenite,Moustafa kamil tombs (M)	4.8 3.0 2.1

Rock weathering class	Degree	Linear crack density (crack/mm)	Rock type code
Sound	I	< 1.5	COM
Slightly weathered	II	1.5–3.0	COM
Moderately weathered	III	3–4.5	COM,M,SH
Weathered	IV	4.5–6	M,SH
Highly weathered	V	6	SH

Table 9 Types of primary and secondary porosity

Types of Rock	Type of porosity	
	primarySecondary	
Sedimentary	Void spaces between mineral grains and bedding planes	Macro and micro fractures (fracture porosity) Solution cavities (vugular porosity) dissolution of a preexisting constituents such as rock fragment,shell or grain (moldic porosity)
Volcanic	Vesicles cooling fractures (columnar joints in basalts) Void spaces in pyroclastic rocks, void spaces in pumice	Macro and micro fractures (fracture porosity) Dissolution of minerals due to weathering
Plutonic	Cooling fractures	Macro and micro fractures (fracture porosity) dissolution of minerals due to weathering

Table 10 Micro porosity %, BET, TPV, nm, specific surface, water absorption coefficient W, saturation coefficient S, for the collected weathered / unweathered rock samples from the sites under investigation

Rock type	BET (m^2/gr)	TPV(ml/gr)	nm	Micro porosity (%)	Specific surface m^2/g	Saturation Coefficient, S	Water absorption coefficient kg/m^2 $h^{0.5}$
Intact calcarenite (El-shatbi tombs) (weathered)	2.38659	0.01472	2.44596 E-05	2.98523	1.5	0.85	1.6
Intact calcarenite (El-shatbi tombs (unweathered	2.46399	0.01186	2.52529 E-05	2.41793	1.3	0.80	1.7
Intact calcarenite (Moustafa kamil tombs) (weathered)	2.79748	1.48453	2.86707 E-05	74.32496	1.4	0.90	1.9
Intact calcarenite (Moustafa kamil tombs, Unweathered	2.15777	0.00749	2.21145 E-05	1.43966	1.3	0.86	2.1
Fossiliferous sandy Oolitic limestone (kom El-Shoqafa, unweathered)	1.51452	0.00232	1.5522 E-05	0.42542	1.9	0.82	1.4
Fossiliferous sandy Oolitic limestone (kom El-Shoqafa) weathered)	2.21098	0.00992	2.26599 E-05	1.79327	1.7	0.90	1.6

in triaxial tests at various confining pressures. Failure envelope and strength parameters of sandy oolitic limestone, Mohr circles diagram from quick –undrained tests as shown in Fig 25. The results of undrained triaxial tests on Calcerinitic rocks, principal stress ratio versus volumetric and axial strain are represented in Fig 26. The results of undrained triaxial tests and the volumetric strain versus axial strain are shown in Fig 27. Figure 28. represents the Typical results of triaxial tests. Young's modulus as a function of confining stress also represented in Fig 29. Deviatoric stress q, versus axial strain ε1 curve, completely weathered rock sample (soil like material) from the main well of Catacomb of Kom El-Shoqafa is shown in Fig 30. The Maximum shear stress T, versus mean effective stress S curve, completely weathered rock sample from the main well of Catacomb of Kom El-Shoqafa is shown in Fig 31, and the Pore pressure, versus axial strain curve, completely weathered rock sample (soil like material) from the main well of Catacomb of Kom El-Shoqafa is well shown in Fig 32. Table 11 summarizes the findings and main results from the short-term laboratory tests carried out on Calcarenitic rock samples under investigation. The result revealed that the sandy Oolitic limestone samples which collected from Catacomb of Kom El-Shoqafa have very low shear strength parameters with poor geotechnical properties of about cohesion c = 500 kN/m^2, friction angle ϕ = 36o, Young,s modulous E = 270 to 360 MPa, Poisson ration ν = 0.26–0.29, shear modulous G = 140.6 MPa, bulk modulous K = 272.7 MPa. For the collected sandy limestone samples collected from El-Shatbi Necropolis the shear strength values also were low where the c = 700 KN/m^2, ϕ = 53°, E = 392 to 445 MPa, ν = 0.24–0.28, G = 172.5 MPa, K = 353.2 MPa. For the Calcarenite collected samples from Mustafa Kamil Necropolis the shear strength value were less

Table 11 Short-term laboratory tests carried out on Calcarenitic, limestone under investigation

Type of rock	Site	N. of sample	γ_d Mg/cm^3	(GS)	η %	Uniaxial compression test				Triaxial compression test						Direct Shear test on rock joints		Brazilian test (BTS) MPa	Block punch index (BPI)	Wave velocity (Vp) Km/sec
						σ_{ucs} MPa	Failure Strain E_f (%)	E Young's Modulus (MPa)	ν [-] Poisson's ratio	φ [o]	C KN/m^2	E Young's Modulus (MPa)	ν [–] Poisson's ratio	{G} Shear modulus (MPa)	{K} Bulk modulus (MPa)	φ [o]	C MPa			
Intact Calcarenite rock (pure Limestone)	*Moustafa kamil necropolissite*	*M_1*	1.62	2.74	36	3.55		68	0.28	31°	400	410	0.28	160	311	56	0	0.37	0.7	1.96
		M_2	1.75	2.80	28	3.45		106	0.30			340	0.28	133	285			0.35	0.7	2.08
		M_3	1.77	2.79	19	2.30		78	0.24			300	0.30	117	227			0.34	1	2.1
		M_4	1.65	2.67	28	3.40		106	0.30									0.34	0.9	2.18
		M_5	1.65	2.84	27	3.45		80	0.28									0.39	1.2	2.48
Sandy oolitic limestone	*Catacomb of komEl-shoqafa*	*COM_1*	1.69	2.66	32	2.6		74	0.24	36°	500	360	0.29	141	273	50	0	0.25	0.5	1.93
		COM_2	1.70	2.78	31	2.74		102	0.28			345	0.26	135	261			0.27	0.6	1.96
		COM_3	1.68	2.49	21	2.7		74	0.28			270	0.26	105	205			0.28	0.7	1.97
		COM_4	1.65	2.80	40	2.6		74	0.24									0.31	1.1	2.06
		COM_5	1.68	2.74	31	2.74		80	0.24									0.29	1	2.17
Oolitic intraclastic limestone	*El-shatbi necropolissite*	*SH_1*	1.80	2.58	23	6.3		147	0.30	53°	700	445	0.28	173	353	62	0	0.46	0.8	2.44
		SH_2	1.79	2.82	23	4.7		138	0.28			440	0.28	172	333			0.49	1	2.55
		SH_3	1.84	2.58	36	5.03		142	0.28			392	0.25	153	297			0.48	1.2	2.71
		SH_4	1.62	2.49	16	6.3		147	0.30			353	0.24	138	267			0.52	1.4	2.83
		SH_5	1.82	2.55	24	6.1		140	0.30			233	0.25	91	177			0.60	1.3	3.06

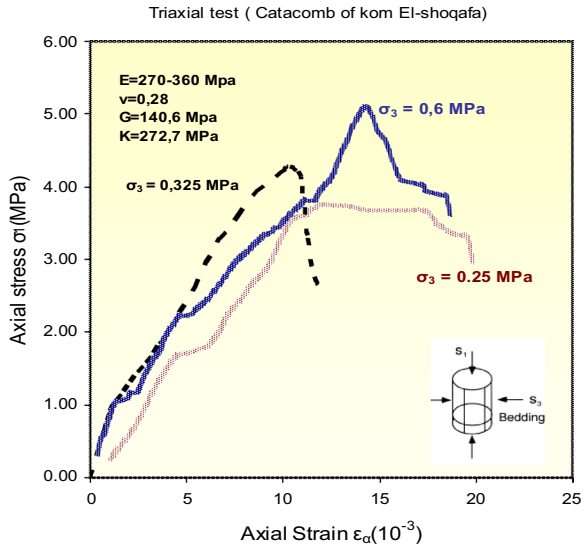

Fig. 18 Stress–Strain curves in triaxial tests at various confining pressures. Catacomb of Kom El-Shoqafa site

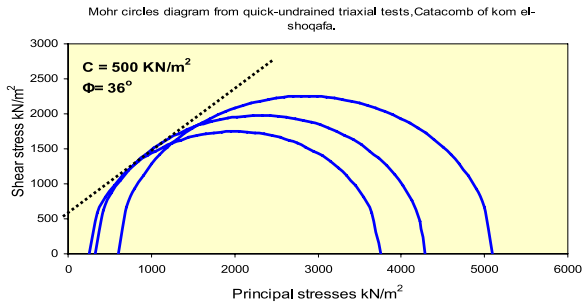

Fig. 19 Failure envelope and strength parameters of sandy oolitic limestone, Mohr circles diagram from quick –undrained tests, Catacombs of Kom El-Shoqafa

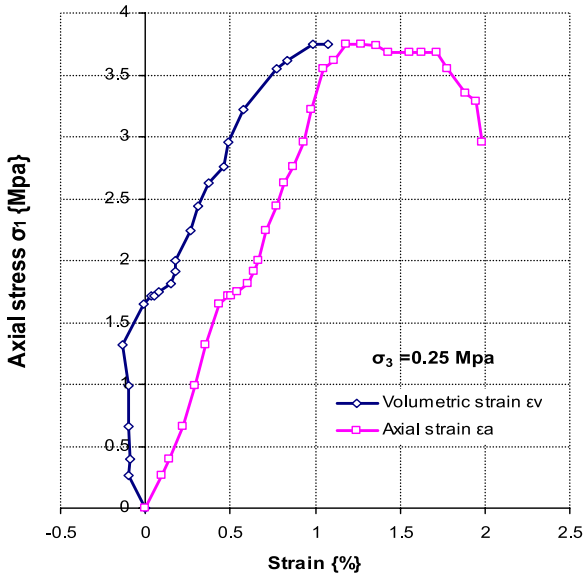

Fig. 20 Results of undrained triaxial tests on sandy oolitic limestone from Catacombs of Kom El-Shoqafa, principal stress ratio versus volumetric and axial strain

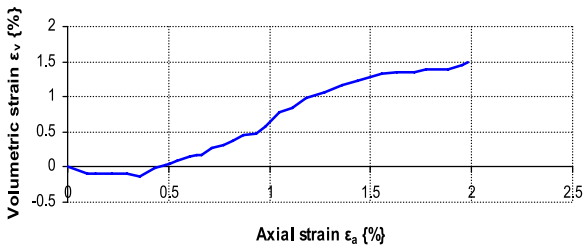

Fig. 21 Results of undrained triaxial tests on sandy oolitic limestone from Catacombs of Kom El-Shoqafa, volumetric strain versus axial strain

than the other two sites where c = 400 KN/m^2, ϕ = 31o, E = 300 to 410 MPa, ν = 0.28–0.30, G = 160.2 MPa, K = 310.6 MPa.

In all the tests the material contracted since the beginning of the application of deviatoric stress; no dilatancy was observed. It is obvious that the peak at low confining pressures is only due to interparticles bonds, as already observed on other soft rocks with high values of porosity.

The different degree of destruct ration obtained, it is possible that the destruct ration consists in the destruction of both the cement, which connects the grains and the grains themselves, and the degree of destruct ration is related to the maximum confining pressure applied to the specimens.

The Triaxial compression test revealed the existence of well-defined yield surfaces. Such yield surfaces are similar in shape to those found in other geomaterials due to overconsolidation and/or the presence of microstructure. As described by [40, 42, 43], a loss of stiffness is noted because of breakage of particle bonds; this loss of stiffness can be observed on the stress–strain curve of each test and is associated with the yield point. Each yield point then represents structural damage caused by loading of the rock specimen.

At high confining pressure, the behavior was ductile, straining beyond yield point took place under constant stress conditions until considerable contract, and volumetric strain had occurred resulting in a significant reduction in void ratio. Thereafter the behaviour was

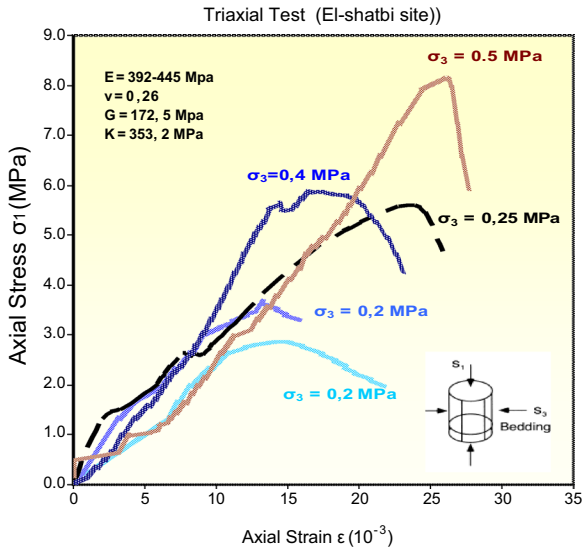

Fig. 22 Stress–Strain curves in triaxial tests at various confining pressures. El-Shatbi Necropolis site

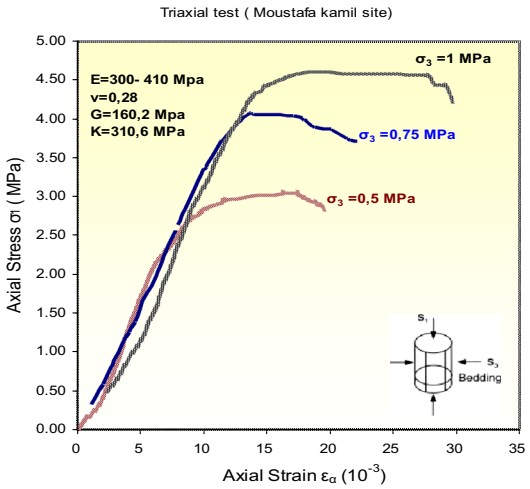

Fig. 24 Stress–Strain curves in triaxial tests at various confining pressures. Necropolis of Mustafa Kamil

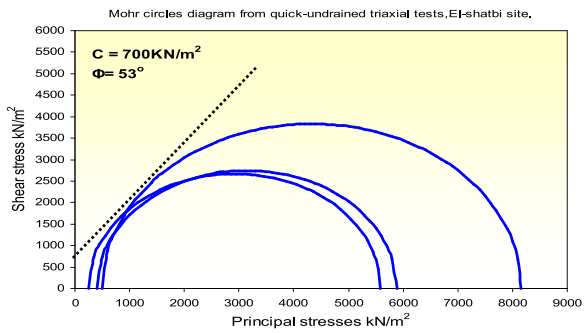

Fig. 23 Failure envelope and strength parameters of oolitic intraclastic limestone, Mohr circles diagram from quick –undrained tests, El-Shatbi Necropolis site

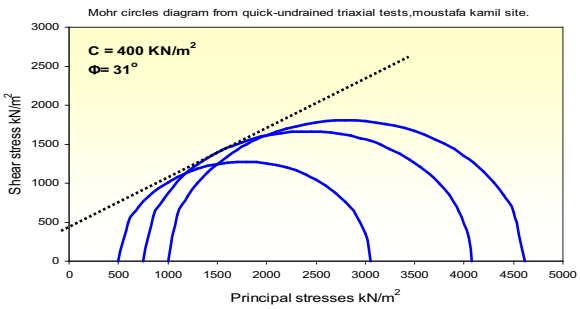

Fig. 25 Failure envelope and strength parameters of intact Calcarenite, Mohr circles diagram from quick–undrained tests, Mustafa Kamil Necropolis site

similar to that of granular materials with crushable particles see e.g. [44, 45].

Large volumetric compression took place in specimens sheared at high effective confining pressure, whilst dilatants behaviour occurred at low pressures.

To summarize, here are important elements of the mechanical behavior of Calcarenitic rocks under investigation:

(I) Although inelastic strains may dominate the stress–strain relationships of soft rocks, elastic behavior is present and may be used for stress measurements using strain recovery techniques.

(ii) This elasticity is eventually nonlinear and anisotropic due to the possible presence of micro cracks.

(iii) Heterogeneity also characterizes the deformability of many soft rocks at the grain scale, which is comparable to the strain gauge scale used in stress measurements.

The variation of the secant Young's modulus in the deviatoric loading stage with different values of σ_3 is also worth examining. Although the data scatter is large, the Young's modulus increases with the confining stress up to a maximum and then it decreases. This fact suggests that isotropic loading above a certain stress level may damage the rock (sample) structure as suggested by [46], this hypothesis seems to be in

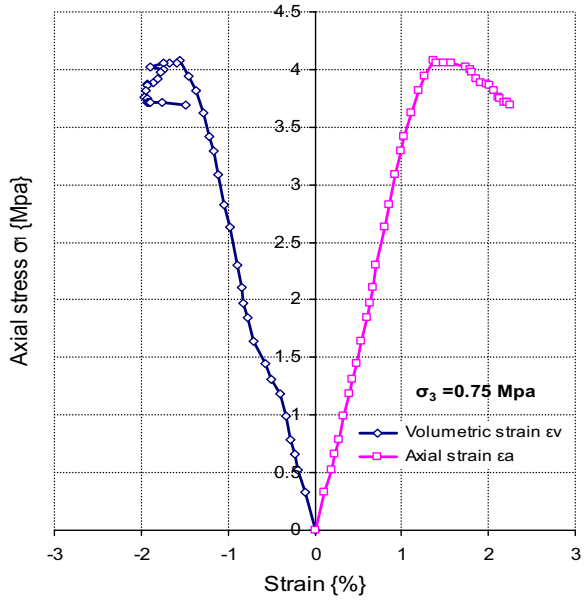

Fig. 26 Results of undrained triaxial tests on Calcerinitic rock from Necropolis of Mustafa Kamil, principal stress ratio versus volumetric and axial strain

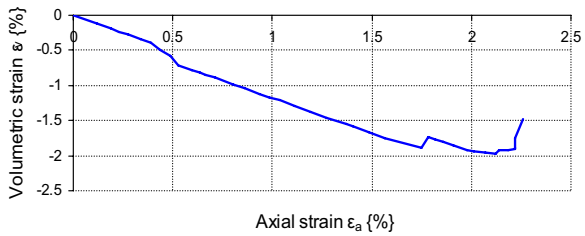

Fig. 27 Results of undrained triaxial tests on calcerinitic rock from Necropolis of Mustafa Kamil, volumetric strain versus axial strain

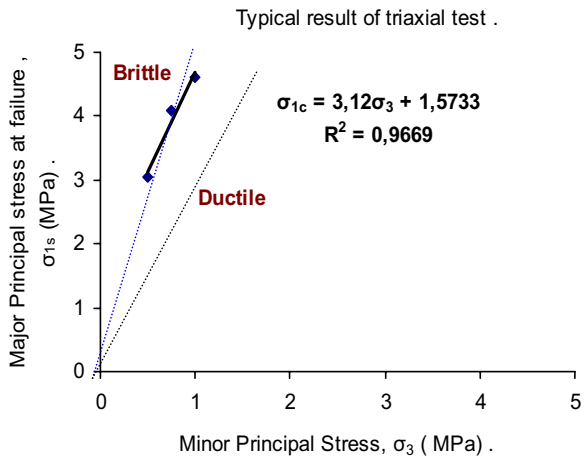

Fig. 28 Typical results of triaxial tests, Mustafa Kamil Necropolis site

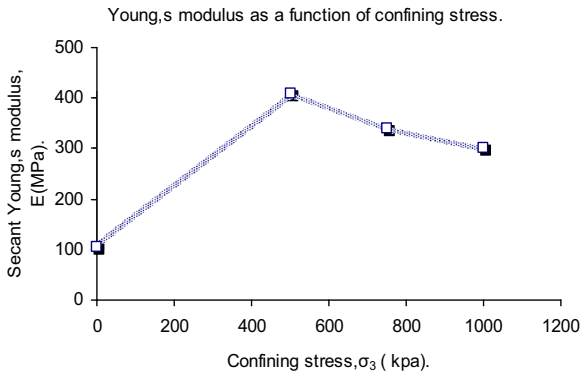

Fig. 29 Young's modulus as a function of confining stress. Mustafa Kamil Necropolis site

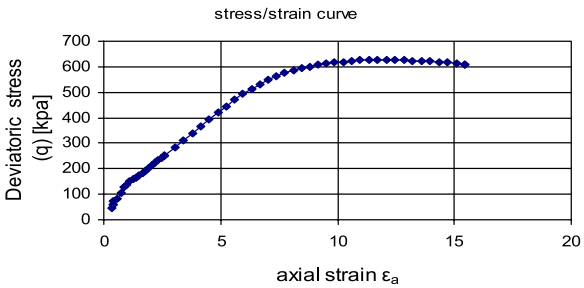

Fig. 30 Deviatoric stress q, versus axial strain ε1 curve, completely weathered rock sample (soil like material) from the main well of Catacomb of Kom El-Shoqafa

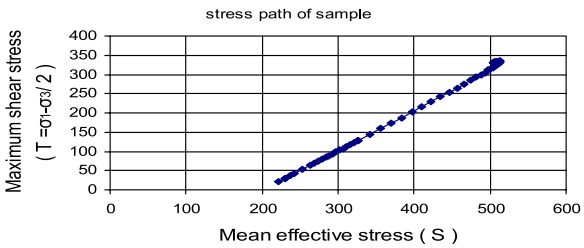

Fig. 31 Maximum shear stress T, versus mean effective stress S curve, completely weathered rock sample from the main well of Catacomb of Kom El-Shoqafa

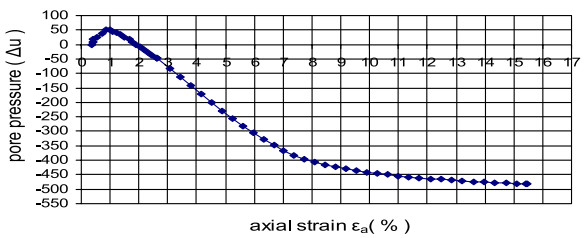

Fig. 32 Pore pressure, versus axial strain curve, completely weathered rock sample (soil like material) from the main well of Catacomb of Kom El-Shoqafa

agreement with the variation of the bulk modulus K with the isotropic stress σm.

Damage to the structure at hydrostatic stresses larger than these corresponding to the brittle-ductile transition, is shown by a decrease of the young's modulus in the deviatoric loading stage.

In Triaxial conditions, the young's modulus shows a gradual decrease up to a normalized deviatoric stress level of 75%; at higher stresses, a rapid drop occurs.

As pointed out first by [47], the particular structure of pyroclastic soft rocks characterize their mechanical behaviour.it can be noticed that, silica percentage in the site of Catacomb of Kom El-Shoqafa is higher in comparison with any area in Alexandria, it may be due to depositional processes, such high silica content that not a cement but found as sand grains, result in decreasing rock durability and hardness, and such high sand grain content reduce rock strength against salt crystallization and hydration pressures within rock pores. This is not only due to its high silica grains content but also as it is sparitic rock. Such limestone type is known to be with low durability, [48, 49].

Brazilian splitting tensile strength (BTS, σ_t)

The Brazil splitting tension tests were included as they gave the tensile strength (σ_t) values comparable to those from the more reliable uniaxial tests. The tensile strength (σt) test provides an index value that is useful for strength classification of rock material, [50, 51]. Totally 33 core specimens obtained from the blocks in vertical direction were used to determine their tensile strength by the Brazilian indirect method. When the rock specimens taken from the three sites are separately considered, and the test was conducted on the specimens by loading rock discs until failure occurs across the diametrical axes [52]. The tensile strength of the Calcarenitic rock from El-Shatbi Necropolis seems to be slightly greater than those from Catacomb of Kom El-Shoqafa and Mustafa Kamil Necropolis.

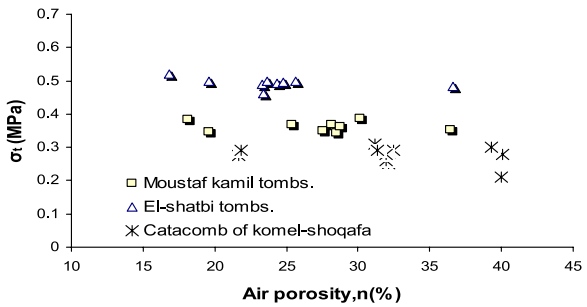

Fig. 33 Tensile strength σt from Brazil tests versus air porosity (n)

For the collected sandy oolitic limestone rock samples from Catacomb of Kom El-Shoqafa, The Brazilian tensile strength (BTS) values ranged from 0.25 to 0.29 MPa and the mean strength were 0.27 MPa at a standard deviation of 40 kPa. And the Calcarenitic rock samples from El-Shatbi Necropolis values ranged from 0.46 to 0.6 MPa with the mean strength was calculated to be 0.53 MPa at a standard deviation of 20 kPa, and for the Calcarenite samples collected from Mustafa Kamil Necropolis values ranged from 0.37 to 0.39 MPa with the mean strength was calculated to be 0.38 MPa at a standard deviation of 25 kPa.

The Young's modulus (E) and Poisson's ratio (v) in Brazilian splitting tension test can be calculated by measuring the strain at the center of the disc in both vertical and horizontal directions. The strain gauge Rosette placed at the center of the disc is best suited for the purpose with the Rosette axis placed parallel and at right angles to the load axis. The relationships for discs (plane stress case) are given by.

The relationships derived above assume that the proportion are the same in compression and tension is however not true for most of the rocks.

Since the stress very throughout the specimen, it is essential that gauges be as small as possible. The gauge length should not be more than 0.07 D for an accuracy of 5%. When strain gauges Rosette are not used and it is

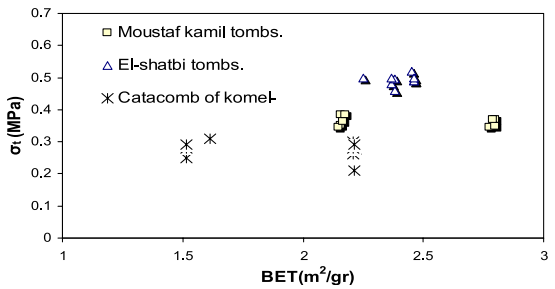

Fig. 34 Tensile strength σt from Brazil tests versus BET

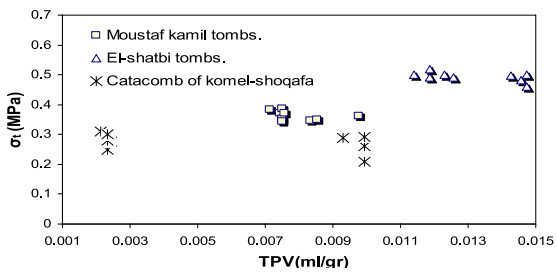

Fig. 35 Tensile strength σt from Brazil tests versus TPV

not possible to place both the strain gauges at the centre.

It is advisable to displace the gauge measuring the radial strain εy along the loaded axis of the disc keeping the gauge measuring tangential strain εx at the centre since the radial strain is fairly constant whereas the tangential strain varies more rapidly [53, 54].

The BTS results reveal that the most of the type rocks considered in this study were of weak to medium according to the ISRM definition.

Figure 33 represents the correlation between the Tensile strength σt from Brazilian tests versus air porosity (n) of the rock samples under investigation.

Figure 34 represents the correlation between the Tensile strength σt from Brazilian tests versus BET of the rock samples under investigation.

Figure 35 represents the correlation between the Tensile strength σt from Brazil tests versus TPV of the rock samples under investigation.

Very slow uniaxial creep test results

Three stages in creep behaviour can be recognized from uniaxial and triaxial creep tests, in the first one, denominated by primary creep, strain occurs at decreasing rate. At some conditions, the primary creep curve approximates a steady rate of strain called secondary creep. In highly stressed specimens, secondary creep may turn upward in tertiary creep, which is characterized by increasing strain rate until creep failure suddenly occurs. In the last two stages diffuse and thin vertical cracking initiates, accompanied by militancy, and, only near to failure, larger cracks propagate rapidly and lead to sudden collapse. Long term tests carried out on specimen's revealed secondary creep showing even at 40% of the estimated strength.

Conclusion

In general, alveolar weathering and impact of marine environment is an often and well described weathering phenomenon in nature as well as on building stones. Nevertheless, dynamics and causes of this particular weathering process are still under discussion. These three archaeological sites (Catacombs of Kom El-Shoqafa, El-Shatby and Moustafa Kamil Tombs) presented an excellent object for a case study on causes and processes of alveolar weathering and impact of climate change and marine environment on world culture heritage.

Within the current research, many studies have been carried out using experimental and laboratory investigations to assess the construction materials durability affected by the marine weathering conditions in the Mediterranean basin. Moreover, these tests have been widely used to evaluate stone durability produced by other decay mechanisms, such as frost action and wetting and drying cycles.

Catacombs of Kom El-Shoqafa and Amod El-Sawari sites which are in the centre of the city, 2.5 km from the sea shoreline, are carved into the oolitic sandy limestone (calcareous cemented sand); they consist of yellowish white massive, fine to medium grained cross-bedded sandstone cemented with calcareous cement. Intersected conjugated joints are filled with very fine friable sand saturated with water in the lower parts. This unit is underlined by loose calcareous sandstone. It consists of brownish medium to fine grained calcareous limestone over saturated with ground water. It overlies the El Hagif formation (Pliocene) or the older Miocene. Surface quaternary deposits obscuring actual contact. The other two archaeological sites, which are close to the waterfront of Alexandria (El-Shatby Necropolis, Moustafa Kamil Necropolis), are excavated in Oolitic intraclastic or calcareinitic limestone (Coastal ridge) with yellowish white colour upwards changing to brownish yellow downwards.

Based on the mechanical testing on dry and wet Calacrenetic rock specimens prepared in vertical direction, the values of uniaxial compressive strength (UCS) indicated that these Calcarenitic rocks within which the underground monuments are excavated, are classified as weak to very weak soft rocks, according to the classification adopted by the geological society of London (1970) which based on unconfined compression strength, and the classification proposed by International Standard of Rock Materials (ISRM) [54]. Also it is in good agreement with the (RQD) rock quality designation system for these kinds of soft rock, where RR = 18 and RQD = 15–20% and the very poor quality range from 0 to 25. In addition, the results of the static deformability tests suggest that the rocks types under investigation have high deformability.

It can be noticed that silica percentage in the site of Catacomb of Kom EL-Shoqafa is higher in comparison with any area in Alexandria, it may be due to depositional processes. Such high silica content that not a cement but found as sand grains, result in decreasing rock durability and hardness, and such high sand grain content reduce rock strength against salt crystallization and hydration pressures within rock pores. This is not only due to its high silica grains content but also because it is sparitic rock. Such soft rock type is known to be with low durability.

The weathering process is linked to the textural characteristics, like poor geotechnical properties, chemical carbonated composition, presence of soluble salts in the porous system, marine climate with characteristic humidity and marine spray, underground water.

Acknowledgements
Not applicable.

Author contributions
The author read and approved the final manuscript.

Funding
Open access funding provided by The Science, Technology & Innovation Funding Authority (STDF) in cooperation with The Egyptian Knowledge Bank (EKB). The author confirms that he is not currently in receipt of any research funding relating to the research presented in this manuscript.

Availability of data and materials
Not applicable.

Declarations

Competing interests
The author declare that he has no competing interests.

Author details
[1]Conservation Department, Faculty of Archaeology, Cairo University, Giza, Egypt.

Received: 13 October 2022 Accepted: 30 April 2023
Published online: 06 June 2023

References

1. El-Sayed MK. Implications of climate change for coastal areas along the Nile Delta. J Environ Prof. 1991;13:59–65.
2. Stanley DJ, Goddio F, Jorstad TF, Schnepp G. Submergence of ancient Greek cities off Egypt's Nile Delta—a cautionary tale. GSA Today. 2004;14:4–10.
3. Abou-Mahmoud MME. Assessing coastal susceptibility to sea-level rise in Alexandria Egypt. Egypt J Aquatic Res. 2021;47(2):133–41.
4. Mai G, Hu Y, Gao S, Cai L, Martins B, Scholz J, Gao J, Janowicz K. Symbolic and subsymbolic GeoAI: geospatial knowledge graphs and spatially explicit machine learning. Trans GIS. 2022. https://doi.org/10.1111/tgis.13012,26,8,(3118-3124).
5. https://www.unesco.org/en/articles/tsunami-resilience-unesco-will-train-100-risk-coastal-communities-2030
6. Randazzo L, Paladini G, Venuti V, Crupi V, Ott F, Montana G, Ricca M, Rovella N, La Russa MF, Majolino D. Pore structure and water transfer in Pietra d'aspra limestone: a neutronographic study. Appl Sci. 2022;10:6745.
7. Rahmouni A, Boulanouar A, BoulanouarMohamed M, et al. Relationships between porosity and permeability of calcarenite rocks based on laboratory measurements. J Mater Environ Sci. 2014;5(3):931–6.
8. Shaaban NA. Water quality and trophic status of Lake Mariut in Egypt and its drainage water after 8-year diversion. Environ Monit Assess. 2022;194:392.
9. Frihy O, Mohamed S, Abdalla D, et al. Assessment of natural coastal hazards at Alexandria/Nile Delta interface. Egypt Environ Earth Sci. 2021;80:3.
10. Dawod GM, Amin AM, Haggag GG. Variations of sea levels and atmospheric parameters along the Egyptian coasts over 2008–2020. J Sci Eng Res. 2022;9(5):85–100.
11. Abdelaali R, Flrhaffari Y. Microstructural characterization by high-energy radiation of porous materials used in civil engineering. IMSEGEC'18 2nd International Material Sciences and Engineering for Green Energy Conference. 2018.
12. Ceraldi TS, Green D. Evolution of the South Atlantic lacustrine deposits in response to early cretaceous rifting, subsidence and lake hydrology. In: Ceraldi TS, Hodgkinson RA, Backe HG, editors. Petroleum geoscience of the west africa margin. London: Geological Society, Special Publications; 2016.
13. Herlinger R Jr, Zambonato EE, de Ros LF. Influence of diagenesis on the quality of lower cretaceous pre-salt lacustrine carbonate reservoir from Northern Campos Basin, offshore Brazil. J Sediment Res. 2017;87:1285–313.
14. Zhao H, Ning Z, Zhao T, Zhang R, Wang Q. Efects of mineralogy on petrophysical properties and permeability estimation of the upper Triassic Yanchang tight oil sandstones in Ordos Basin. Northern China Fuel. 2016. https://doi.org/10.1016/j.fuel.2016.08.096.
15. Atwa SM. Hydrology and hydrogeochemistry of the northwestern Coast of Egypt. Egypt: PhD Dissertation, Faculty of Science University of Alexandria, Alexandria; 1979.
16. El-Fiky, A.A., Fattah, Th. A. Abdel, and M.H. Farag. Geophysical investigations in study groundwater in the northwestern coastal zone, Egypt. paper presented at the 2002 seg annual meeting, Salt Lake City, Utah, October 2022.
17. Abd El Mawla, S.H. Stability of natural grounds Geology, geomorphology, seismology and tsunami. THE WORLD BANK Climate Change Adaptation and Natural Disasters Preparedness in the Coastal Cities of North Africa Phase 1 : Risk Assessment for the Present Situation and Horizon 2030 – Alexandria Area National Workshop – Alexandria. 2010.
18. Frihy OES, Deabes EA, Shereet SM, Abdalla FA. Alexandria-Nile Delta coast, Egypt: update and future projection of relative sea-level rise. Environ Earth Sci. 2010;61(2):253–73. https://doi.org/10.1007/s12665-009-0340-x.
19. Stanley JD, Clemente PL. Increased land subsidence and sealevel rise are submerging Egypt's Nile Delta coastal margin. GSA Today. 2017;27(5):4–11. https://doi.org/10.1130/GSATG312A.1.
20. Yalciner AC, Zaytsev A, Aytore B, Insel I, Heidarzadeh M, Kian R, Imamura F. A possible submarine landslide and associated tsunami at the northwest Nile delta. Mediterranean sea Oceanogr. 2014;27(2):68–75. https://doi.org/10.5670/oceanog.2014.41.
21. Radwan AA, El-Geziry TM. some statistical characteristics of surges at alexandria. Egypt J King Abdulaziz University: Marine Sci. 2013;179(1791):1–17.
22. El-Quilish M, El-Ashquer M, Dawod G, El Fiky G. Development and accuracy assessment of high-resolution digital elevation model using GIS approaches for the Nile Delta Region Egypt. Am J Geograp Inform Sys. 2018;7(4):107–17. https://doi.org/10.5923/j.ajgis.20180704.02.
23. Dawod G, Mohamed H, Haggag G. Relative and absolute sea level rise based on recent heterogeneous geospatial data: a case study in the Nile delta Egypt. J Scient Eng Res. 2019;6:55–64.
24. Mohamed HF, Bahaa AS, Magdy MH, Gomaa MD. High precision GPS monitoring of the land subsidence in the Nile Delta: status and preliminary results. Sharm El-Sheikh: Regional conference on surveyingg & Development; 2015.
25. Hasan E, Khan SI, Hong Y. 2015. Investigation of potential sea level rise impact on the Nile Delta Egypt using digital elevation models. Environ Monitor Assess. 10 1007/s10661-015-4868-9
26. Ali EM, El-Magd IA. Impact of human interventions and coastal processes along the Nile Delta coast, Egypt during the past twenty-five years Egypt. J Aquat Res. 2016;42(1):1–10. https://doi.org/10.1016/j.ejar.2016.01.002.
27. Lima MCO, Pontedeiro EM, Ramirez MG. Impacts of mineralogy on petrophysical properties. Transp Porous Med. 2022;145:103–25. https://doi.org/10.1007/s11242-022-01829-w.
28. Rives V, García-Talegón J. Decay and conservation of building stones on cultural heritage monuments. Switzerland: Trans Tech Publications; 2006.
29. Vicente MA, Vicente-Tavera S. Clays. Clay Miner. 2001;49:227.
30. Shreadah MA, El-Rayis OA, Shaaban NA, Hamdan AM. Water quality assessment and phosphorus budget of a lake (Mariut, Egypt) after diversion of wastewaters effluents. Environ Sci Pollut Res. 2020;27(21):26786–99.
31. Doehne E. Salt weathering: a selective review. Geol Soc London. 2002. https://doi.org/10.1144/GSL.SP.2002.205.01.05.
32. Arnold A, Zehnder K. Salt weathering on monuments. Advanced Workshop. Analytical methodologies for the investigation of damaged stones. Pavia, Italy, Sept 14–21, 1990, organized by F Veniale and U Zezza, 58 pp
33. Zehnder K. New aspects of decay caused by crystallization of gypsum, conservation of stone and other materials edit. Paris: RILEM, causes of disorders and diagnosis; 1993.
34. Ashton SA. Ptolemaic Alexandria and the Egyptian tradition. In: Hirst A, Silk M, editors. Alexandria, real and imagined. Abingdon-on-Thames: Routledge; 2004.

35. Basheer AA, Kamis Q, Moahmed A. Geophysical investigation to reveal the groundwater condition at New Borg El-Arab industrial city. Egypt NRIAG J Astron Geophys. 2014;3(2):117–29.
36. El-Sayed A, Korrat I, Hussein HM. Seismicity and seismic hazard in Alexandria (Egypt) and its surroundings. Pure Appl Geophys. 2004. https://doi.org/10.1007/s00024-003-2488-8.
37. Chalari A, Papatheodorou G, Geraga M, Christodoulou D, Ferentinos G. A marine geophysical survey illustrates Alexandria's Hellenistic past. Zeitschrift fur Geomorphologie. 2009;53(1):191–212.
38. El Assal M. Geomorphology and geoarchaeology of Alexandria, Ph.D. thesis, Faculty of Arts, Damanhour University, Egypt & Aix En Provence University, France. 2013.
39. AbuoelelaMojame A, et al. Effects of surface geology on the ground-motion at New Borg El-Arab City, Alexandria, Northern Egypt. NRIAG J Astron Geophys. 2016;5(1):55–64.
40. Hemeda S, Sonbol A. Sustainability problems of the Giza pyramids. Herit Sci. 2020;8:8.
41. Brown ET. Risk assessment and management in underground rock engineering—an overview. J Rock Mech Geotech Eng. 2012;4(3):193–204.
42. ASTM Standard C568, C568M. Standard specifcation for limestone dimension stone. West Conshohocken: ASTM International; 2015.
43. Hemeda S, Pitilakis K. Serapeum temple and the ancient annex daughter library in Alexandria, Egypt: geotechnical–geophysical investigations and stability analysis under static and seismic conditions. Eng Geol. 2010;113:33–43.
44. Cecconi M, Viggiani GM. Structural features and mechanical behaviour of a pyroclastic weak rock. Int J Numer Anal Meth Geomech. 2001;25:1525–57.
45. ASTM D7012-10. Standard test method for compressive strength and elastic moduli of intact rock core specimens under varying states of stress and temperatures. West Conshohocken: ASTM International; 2010.
46. Hemeda S. Geotechnical and geophysical investigation techniques in Ben Ezra Synagogue in old Cairo area Egypt. Herit Sci. 2019;7:23. https://doi.org/10.1186/s40494-019-0265-y.
47. Katz O, Reches Z, Roegiers JC. Evaluation of mechanical rock properties using a Schmidt Hammer, Technical Note. Int J Rock Mech Min Sci. 2000;37:723–8.
48. Saptono, S. Pengembangan Metode Analisis Stabilitas Lereng Berdasarkan Karakterisasi Batuan di Tambang Terbuka Batubara. Disertasi Doktor, Rekayasa Pertambangan, Institut Teknologi Bandung. 2012.
49. Hemeda S. Engineering failure analysis and design of support system for ancient Egyptian monuments in Valley of the Kings, Luxor Egypt. Geoenviron Disasters. 2018;5:12. https://doi.org/10.1186/s40677-018-0100-x.
50. Hemeda S. 3D fnite element coupled analysis model for geotechnical and complex structural problems of historic masonry structures: conservation of Abu Serga church, Cairo Egypt. Herit Sci. 2019;7:6. https://doi.org/10.1186/s40494-019-0248-z.
51. ASTM C 805–85. Test for rebound number of hardened concrete. USA: ASTM; 1993.
52. Maximilian H, Jörg K, Marlène V, Nina G, Robert G. A large-scale geomechanical and petrophysical data set measured across the Geneva Basin as part of CERN's FCCIS mining-the-future competition. 2021. Zenodo. https://doi.org/10.5281/zenodo.4725585.
53. ASTM C496, C496M-17. Standard test method for splitting tensile strength of cylindrical concrete specimens. West Conshohocken PA: ASTM International; 2017.
54. ISRM. Suggested methods for determining tensile strength of rock materials part 2: suggested method for determining indirect tensile strength by the Brazil Test. Int J Rock Mech Min Sci. 1978;15:99–103. https://doi.org/10.1016/0148-9062(78)90003-7.

Publisher's Note